

Earth and Space Science

RESEARCH ARTICLE

10.1029/2023EA003145

Potentially Toxic Elements (PTEs) Distribution in Drainage Canal Sediments of a Low-Lying Coastal Area



Key Points:

- First study on Potentially Toxic Elements (PTEs) enrichment in drainage canal sediments of reclaimed low-lying coastal area
- Key roles of (i) Fe- and Mn-oxyhydroxides in PTE enrichments and (ii) salt-derived cations in adsorption efficiency
- Distance from the sea, salinity of drainage water, and use of fertilizers are the main factors affecting the distribution and enrichment of PTEs

Supporting Information:

Supporting Information may be found in the online version of this article.

Correspondence to:

N. Greggio,
nicolas.greggio@unibo.it

Citation:

Giambastiani, B. M. S., Greggio, N., Carloni, G., Molducci, M., & Antonellini, M. (2024). Potentially toxic elements (PTEs) distribution in drainage canal sediments of a low-lying coastal area. *Earth and Space Science*, 11, e2023EA003145. <https://doi.org/10.1029/2023EA003145>

Received 30 JUN 2023

Accepted 19 JUN 2024

Author Contributions:

Conceptualization:

B. M. S. Giambastiani, M. Antonellini

Data curation: B. M. S. Giambastiani, N. Greggio, G. Carloni

Formal analysis: B. M. S. Giambastiani, G. Carloni




Investigation: G. Carloni

Methodology: B. M. S. Giambastiani, N. Greggio

Resources: M. Molducci

Supervision: M. Antonellini

Validation: B. M. S. Giambastiani, M. Molducci

B. M. S. Giambastiani¹ , N. Greggio¹ , G. Carloni^{1,2}, M. Molducci³, and M. Antonellini¹ 

¹BiGeA—Biological, Geological and Environmental Sciences Department at Interdepartmental Centre for Environmental Sciences Research (CIRSA), Alma Mater Studiorum, University of Bologna, Ravenna, Italy, ²Province of Ferrara, Territorial and Urban Planning Office, Ferrara, Italy, ³Consorzio di Bonifica della Romagna, Ravenna, Italy

Abstract This study examines the accumulation, distribution, and mobility of Potentially Toxic Elements (PTEs) in the sediments of a low-lying coastal drainage network (Ravenna, Italy). The aim is to understand the geochemical processes occurring between drainage water and canal bed sediments and assess factors affecting and driving PTE distribution and enrichment in these environments. A geochemical database resulting from the analysis of 203 drainage sediment samples was analyzed using Principal Component Analysis and compared to undisturbed near-surface sediment samples from the same depth and depositional environment. The results reveal PTEs exceeding national regulation limits. Distance from the sea, electrical conductivity of drainage water, and fertilizer use were identified as the main driving factors. The primary mechanisms for PTE precipitation (As, Co, Mo) and subsequent enrichment in the sediments is attributed to the absorption on Fe- and Mn-oxyhydroxides (HFO and HMO), particularly in high salinity areas near the coast. While Cu, Zn, Pb, Cr, and V also have affinity for HFO and HMO, their adsorption efficiency decreases due to the competition with salt-derived cations during ongoing salinization processes. Anthropogenic sources, including agriculture, hunting activities, traffic dust, and railways, contribute to the local abundance of other elements (Cr, Ni, Cu, Zn, Pb, and Sn). This paper's significant progress lies in assessing the concurrent interactions of chemical and physical processes that drive PTE distribution and accumulation in reclaimed low-lying coastal plains. The findings are significant for assessing PTE accumulation risks and sediment toxicity in coastal areas affected by water salinization, drainage, and subsidence, providing valuable information to water management institutions globally.

Plain Language Summary This study investigates the presence of harmful substances called Potentially Toxic Elements (PTEs) in the sediment of the drainage canals in Ravenna's coastal area (Northern Italy). Researchers want to understand how these substances accumulate and spread in the sediment and what factors influence their distribution. They collected sediment samples from the bottom of the drainage canals and compared them to natural sediment samples. The results show that the PTE levels exceed the national and international limits. The distance from the sea, the water salinity, and the fertilizers are found to be the main factors affecting the distribution of PTEs. The researchers also discover that some PTEs (Arsenic, Cobalt, and Molybdenum) are absorbed by certain minerals in the sediment, especially in areas with high salinity close to the coast. However, other harmful elements, like copper, zinc, lead, chromium, and vanadium are not as strongly absorbed due to competition with salt-related substances. The abundance of other elements like chromium, nickel, copper, zinc, lead, and tin come from human activities like agriculture, hunting, traffic, and railways. These findings are important for understanding the risks associated with these substances in the sediment, particularly in low-lying coastal areas that have been reclaimed for human use.

1. Introduction

Potentially Toxic Elements (PTEs), as defined by Pourret and Hursthouse (2019), are a list of inorganic contaminants deriving from anthropogenic sources that represent a global issue because of their persistence and toxicity in the environment. The PTEs are naturally present in the mineral (inorganic) component of the soils with varying concentrations mainly due to the chemical composition of the rock substrate from which the soil originates (Appelo & Postma, 2004). Anthropogenic activities, such as mining, metallurgical industries, fossil fuel combustion (Ahado et al., 2021; Protano et al., 2021; Vareda et al., 2019), and agricultural use of fertilizer and pesticides contribute to an increase in PTEs concentration (Ahmad et al., 2023; Falconer, 1998; Hua et al., 2023).

© 2024. The Author(s).

This is an open access article under the terms of the [Creative Commons Attribution-NonCommercial-NoDerivs License](#), which permits use and distribution in any medium, provided the original work is properly cited, the use is non-commercial and no modifications or adaptations are made.

Writing – original draft:

B. M. S. Giambastiani, N. Greggio,
G. Carloni, M. Antonellini

Writing – review & editing:

B. M. S. Giambastiani, N. Greggio,
M. Antonellini

Where present at high concentrations, such elements interfere with the normal metabolism of plants, animals, and humans (Abdu et al., 2017; Nieder & Benbi, 2023).

Once inorganic pollutants (i.e., Cu, Zn, Pb, Ni, Cd) enter the environment, their availability and fate in soil and water are complex and depends on several physical and chemical parameters such as dissolved organic matter (Abdelrady et al., 2020), salinity (Choi et al., 2020; Du Laing et al., 2008; Jia et al., 2017), soil pH, cation exchange capacity, and oxidation-reduction state of the metals. The pH is important in regulating metal mobilization in soils as high values, that is, due to the use of fertilizers or liming, favor retention and decrease solubility of metal cations (Orhue & Frank, 2011). Among natural particles, Fe and Mn oxy-hydroxides have long been recognized as playing an important role in determining the fate of several PTEs and in controlling trace elements cycling in soils (Franks et al., 2021; Pavoni et al., 2018), streams, groundwater (Orhue & Frank, 2011), and seawater (Colombani et al., 2015; Ferraro et al., 2022), mainly as a function of the pH-Eh parameters, as well as depending on the chemistry of the aqueous phase.

Given that PTEs are not degradable (Adriano et al., 2004), bioaccumulation and biomagnification occur throughout all levels of the food chain, causing different diseases and poisoning (Adriano, 2001; WHO, 2017). Microorganisms are extremely sensitive to PTEs (Giller et al., 1998); elevated concentrations of PTEs in soils decrease soil microbial biomass, diversity, and activities (Abdu et al., 2017) and negatively affect plant growth (Asati et al., 2016). The major effect of PTEs on the ecosystem is bioaccumulation in the tissue of living organisms. For instance, bioaccumulation of Hg, Pb, Cr, Cd, and As are proven to disrupt cellular functions including growth, proliferation, differentiation, and damage-repairing processes (Balali-Mood et al., 2021) and they can cause cancer, respiratory problems, kidney pathology, neurological disorders, and a series of other diseases (Bernhoft, 2012; Sall et al., 2020).

PTEs mobilities, their adsorption and precipitation processes, as well as plant uptake and bioaccessibility have been well characterized and described in land reclamation of mine sites (Fernández-Caliani et al., 2021; Sánchez-Donoso et al., 2021; Viadero, 2019), of agricultural alluvial areas (Mao et al., 2022), but less is known in subsiding coastal reclamation areas (Di Giuseppe et al., 2014; Mollema et al., 2015), and in particular in drainage system sediments, where salinity on clay minerals and organic matter can play an important role in controlling adsorption and fate of PTEs.

In this context, the work investigates the distribution and accumulation of PTEs in sediments of drainage canals from coastal basins located in the south-eastern portion of the Po River plain, along the coastal strip between the city of Ravenna and the coastal municipality of Cesenatico (Figure 1). The area is characterized by low topography (0 to −2 m a.s.l.) and is affected by flooding, subsidence, groundwater and soil salinization (Antonellini et al., 2008, 2019; Gattacceca et al., 2009; Giambastiani et al., 2013, 2020, 2021; Greggio et al., 2020; Orecchia et al., 2022). This area includes territories with different land use, such as agricultural, industrial, natural, and urban coastal areas. The majority of the territory is a reclamation area undergoing mechanical drainage operated by artificial canals and pumping stations that discharge inland water towards the Adriatic Sea. The complex drainage network, managed by the local Land Reclamation Consortium (LRC) is fundamental to controlling the water table, guaranteeing agricultural activity, and avoiding flooding of the territory. Most canals are used both for drainage and irrigation purposes based on seasonality and agricultural needs (Greggio, Giambastiani, & Antonellini, 2018; Greggio, Giambastiani, Campo, et al., 2018). As for a large part of the north Adriatic coastal area, in the past century, gas and groundwater exploitation has caused land subsidence (Teatini et al., 2005) that deeply affected the drainage network requiring new investments and excavations to keep the system working and land dry (Giambastiani et al., 2020). The canal excavation cuts through the most superficial soil layer and into the aquifer deposits to impart an efficient hydraulic gradient towards the pumping station; the canal bottom, however, remains within the same original deposition facies of the aquifer. For this reason, the comparison between the geochemistry of the canal bed sediments and the near-surface sediments of the same facies is possible. Furthermore, we can distinguish element enrichments that have been occurring due to the interaction between drainage water and the sediment itself.

When considering the management of sediment in canals, it is commonly assumed that the focus is on “materials from channel dredging” or sludges originating from coastal infrastructures and industrial harbor maintenance (Bianchini et al., 2019; Soliman et al., 2019). However, there has been limited investigation into the bed sediments of drainage canals. Shi et al. (2021) employed geochemical fingerprints to identify the sediment sources in drains within a small catchment in China; Hassaan et al. (2022) assessed PTE contamination in water and sediments in

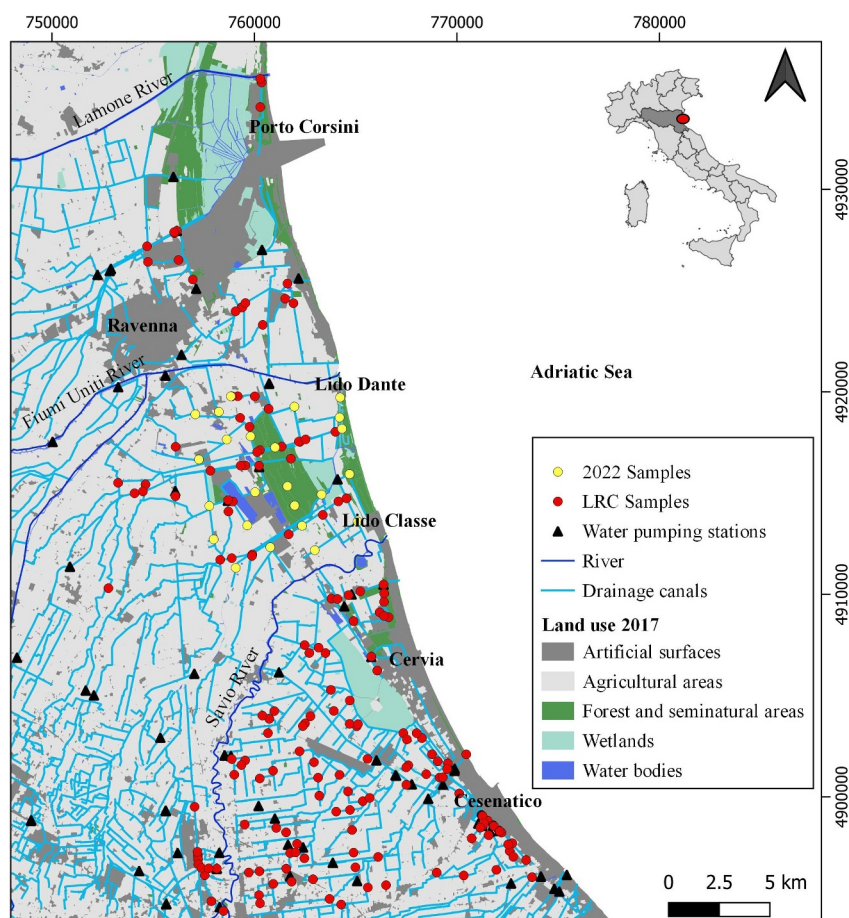


Figure 1. Location of the study area. The complex drainage network, consisting of several water pumping stations (black triangles) and artificial drainage canals (cyan lines), is shown. Also illustrated is the simplified land use (coastal pine forests; agricultural land; and urban areas) and the sediment samples database used for the study: in yellow color samples of the Focus Area, and in red color the LRC database for the entire studied coastal area. (Coordinate Reference system: WGS84/ UTM zone 32N, EPSG: 32632).

the drainage network of Lake Mariot in Egypt; other studies have focused on characterizing mine stream sediments and the migration of PTEs along the drainage network (Friedland et al., 2021; Ghezzi et al., 2021; Prudêncio et al., 2015; Srarfi et al., 2019; Wei et al., 2022). In other cases, sediments from urban waterways have been studied to highlight the geochemical processes occurring upon exposure to the atmosphere during dredging operations (Cook & Parker, 2003). From all these studies it is evident how the distribution of PTEs in natural and artificial water bodies can be influenced by various factors, such as the source of PTEs, morphology, and human activities. However, to the best of the authors' knowledge, there is a complete absence of studies on the abundance and distribution of PTEs in sediments from drainage canal networks, particularly in reclaimed low-lying coastal basins subjected to salinization processes and heavily oriented towards agriculture. If there are such studies, they are generally limited to specific elements or are isolated case studies (Bijlsma et al., 1996; Kelderman et al., 2000). In our work, sediments of the drainage network are characterized in detail and PTEs enrichment processes due to drainage and other human activities are identified. Multivariate statistics are applied to the geochemical data set collected at a coastal basin-wide scale to identify which factors, among the change in drainage water salinity, topography, and fertilizer usage, are the main drivers of PTEs distribution and accumulation. Our findings provide relevant information to land reclamation authorities, which are in charge of irrigation water and management of dredged sediments from the reclamation networks.

2. Characterization of the Study Area

2.1. Hydrogeological Setting

The coastal phreatic aquifer (Figure 2) is composed of Holocene sediments whereas the Pleistocene alluvial clay below constitutes the impermeable bottom confining layer. The aquifer is located within the littoral sands, and locally in the shallow marine wedge deposits (Amorosi et al., 1999; Campo et al., 2017). The shallow coastal aquifer consists of a wedge-shaped dune and beach sand body pinching out in westerly and northerly directions, which is sealed at the bottom and top by clays and peat formed in lagoons, marshes, and alluvial plains. There are two main sand units: a thick medium-grained sand unit at the top of the aquifer (about 10 m in thickness) and a lower fine-grained sand unit of small thickness (≈ 2 m). These two sand bodies are separated in the coastal area by an alternation of clay-silt and sand-silt layers (prodelta) and merge landward where the prodelta disappears. The sand-clay ratio decreases in the western part, toward the agricultural area, where the aquifer mainly consists of recent alluvial plain deposits and back-barrier facies association including fine-grained sediments with abundant organic matter, typical of the lagoon and marsh environments (Amorosi et al., 2008).

The outcropping soils of the study area correspond to recent sedimentary deposits that can be grouped into four association facies based on the depositional environment (Amorosi & Sammartino, 2007; Buscaroli et al., 2009, 2021; RER, 1999a, 1999b): beach ridge deposits (BR) consisting in medium and fine sand with 0.1%–0.5% of organic matter (OM); salt marsh and back ridge lagoon deposits (SM) consisting in silt, sand and fine sand with 0.6%–0.9% of OM; channel, levee and river flooding deposits (CL) of fine and very fine silty sand with 0.3%–0.8% OM; and interfluvial flood-deposits (IF), made of silty clay, clay and laminated clayey silt, in the most inland area with 0.7%–1% OM. As shown in Figure 2, the study area is dominated by sediments belonging to the BR facies association, interspersed with fine sediments of alluvial origin belonging to the CL facies association. BR deposits constitute the phreatic coastal aquifer, whereas CL sediment partially or completely confines the aquifer.

The coastal area is drained constantly so that the water table is about 1–1.5 m below ground level during the entire year. The drains are excavated in the near-surface sediments of the coastal deposits. To maintain adequate hydraulic gradient, canals are about 3–4 m deep close to pumping stations and shallower (about 1–2 m) as the distance from the pumping stations increases. Pumping creates a general inland-directed hydraulic gradient, a decrease in the effective recharge of the aquifer, and a vertical hydraulic gradient that forces saline groundwater to flow upward from the bottom of the aquifer (Figure 2) (Giambastiani et al., 2020). Land subsidence, varying from 2.5 to 20 mm/year, has led to the rise of the water table in the shallow unconfined aquifer that has consequently required a progressive increase in pumping drainage rates through time to avoid flooding of large coastal areas (Antonellini et al., 2019). The cumulative total increase of annual drainage over the period 1988–2017 is estimated to be 150 mm (total volume divided by the area of the coastal basin, Giambastiani et al., 2020), whereas the amount of freshwater that infiltrates into the aquifer is around 14 mm/year (Antonellini et al., 2008), resulting in limited effective recharge and imbalance between winter surplus and summer deficits (Benini et al., 2016) that favors saltwater intrusion.

2.2. Sediment Geochemistry

In general, the natural composition of sediments of BR association facies (Figure 2) is characterized by a high content of SiO_2 and CaO and low content of Al_2O_3 , Fe_2O_3 , K_2O , TiO_2 , and OM. Also trace elements such as V, Rb, Br, Cu, Zn, and Y are poor and only Ni and Cr show some local enrichments. Having been deposited during the last progradation period, the origin of these sediments depends on river supply: the oldest sediments (>1,000 years BP) show a typical alpine provenance (Po river origin with high Cr and Ni concentration), whereas the youngest ones have a clear Apennine origin (by Apennine rivers, with low Cr and Ni concentration) (Greggio, Giambastiani, & Antonellini, 2018; Greggio, Giambastiani, Campo, et al., 2018).

The high presence of silt and organic material of CL association facies leads to an abundance of Al_2O_3 and Fe_2O_3 . Based on different ratios of Cr, Ni, CaO, and Sr, Amorosi and Sammartino (2007) attribute the origin of near-surface sediments to the Apennines, in which CaO and Sr are the most abundant components.

The recent work by Buscaroli et al. (2021) completes and confirms the results of Amorosi and Sammartino (2007). Indeed, they report that V, Fe, Al, Mg, Ti, Ni, Co, Rb, Y, Nb, K, La, Cr, Zr, LOI (Loss on Ignition, representing the amount of organic matter in the sample) characterize the near-surface alluvial plain sediment (CL); in particular, V, Zn, Rb, Fe, La, Co, K and Al have positive correlations with fine particle size. In BR

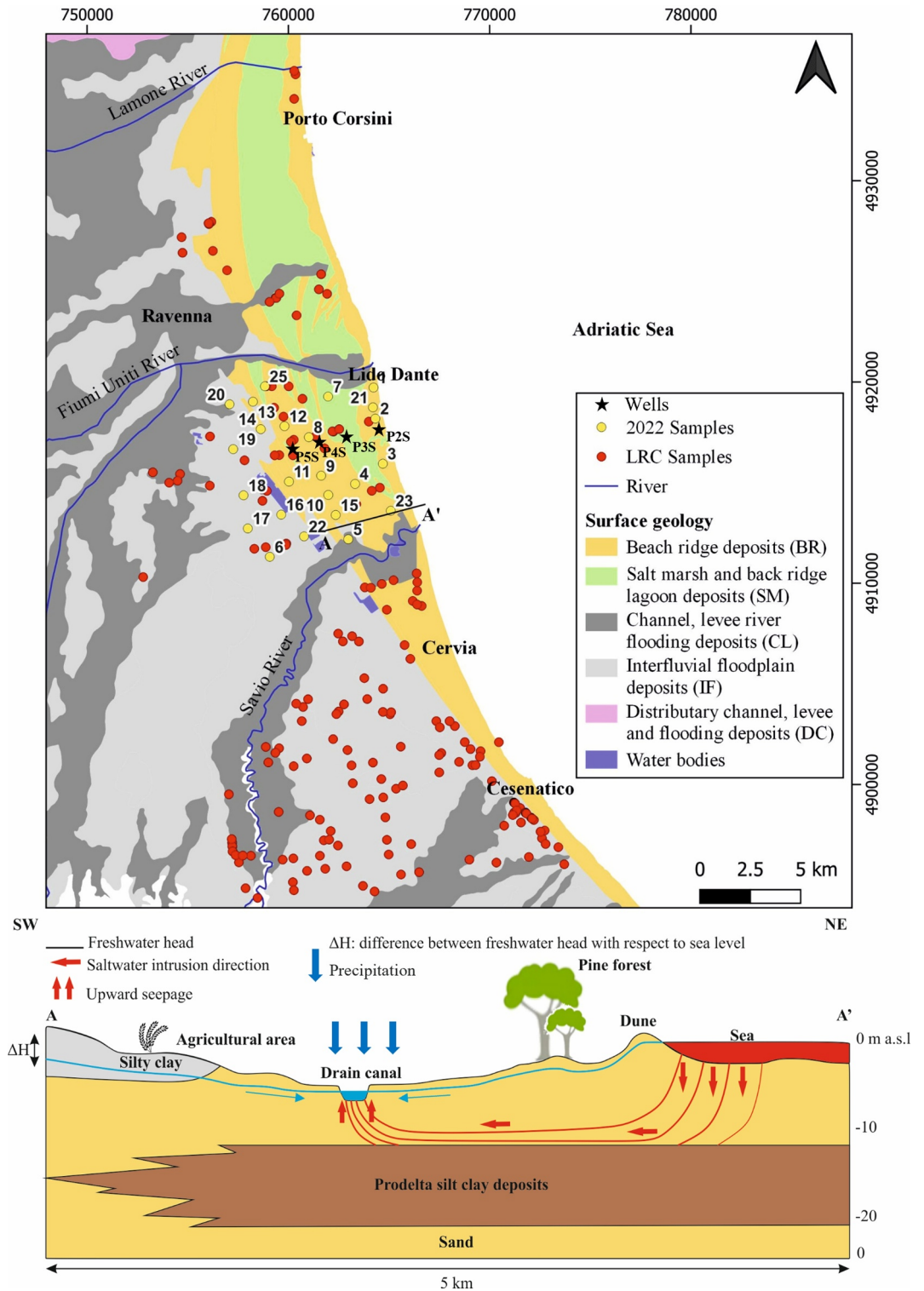


Figure 2. Surface geology map (modified from RER - Emilia-Romagna Region (1999a, 1999b), scale 1:50000) showing the depositional environment (a) and the cross-section of the shallow coastal aquifer (b).

samples Sr, LOI, Ca, Ba, Cu, Zn, Pb, and Si are the most abundant, whereas Sr as well as other elements such as Ba, Cu, Pb, and Zn, show affinity with carbonates of Apennine origin.

2.3. Water Geochemistry

In the study area, the hydrochemistry of surface and groundwater is affected by the saltwater intrusion process, cation exchange between water and sediments, dissolution of calcite and gypsum, and redox reactions (Greggio et al., 2020; Kralj, 2012; Mollema et al., 2013). Within the shallow unconfined aquifer, the main water type is brackish to saline with Na and Cl as major cations and anions, respectively. Groundwater salinity ranges from 0.4 to 6 g/l in the most inland part (Antonellini et al., 2008), up to the highest values of 10–20 g/l measured along the coastal pine forests (Cozzolino et al., 2017), with little variation between winter and summer. The source of the salinity is from seepage of connate seawater enclosed in sediments, or current seawater intrusion (Giambastiani et al., 2013; Mollema et al., 2013). The pH is, on average 7.4 and 8.4 for groundwater and river water, respectively (Mollema et al., 2015).

Brackish and saline waters are the dominant types in the pine forests, whereas the variety of groundwater types in the inland agricultural area can be explained by the mixing of precipitation, vertical seepage of Adriatic seawater, and irrigation water from the Po River (Greggio et al., 2020).

High concentrations of Fe, Cr, As, Mn, Al, and Cu are found in groundwater (Petrini et al., 2014), with values that in some cases exceed the legal limits imposed by the Italian regulations (D.Lgs n. 152/2006, 2006) and the WHO guidelines (WHO, 2017). According to Mollema et al. (2015), As concentrations are, on average, 20.2 and 26 µg/L in surface water and groundwater, respectively; As concentrations up to 120 ppb were also found North of Ravenna (Kralj, 2012). Greggio et al. (2020) characterized drainage, river, and ground waters showing that B, Co, Cu, Fe, Mn, and Zn are more concentrated in drainage than river water.

3. Methodology

3.1. Data Acquisition and Database Creation

Since 2010 the LRC has collected a total of 182 sediment samples along the studied drainage system. The samples were collected at the drain bed using an auger and prepared by Aqua regia digestion for analysis through inductively coupled plasma mass spectrometry (ICP-MS) for As, Cd, Cu, Co, Cr, Hg, Ni, Pb, Cu, Zn, Sn, based on the EPA 3051A (U.S.EPA, 2007a) and EPA 6010D (U.S.EPA, 2018) methods and cold-vapor atomic absorption for the total Hg, based on the EPA 7473 method (U.S.EPA, 2007b). Aqua regia digestion is a partial digestion that is used to extract trace elements in soil and sediments and involves treating the sample with a mixture of concentrated nitric and hydrochloric acids. However, this method only represents the portion of the sample that is extracted and does not provide a complete analysis of the sample. The analysis of LRC sediments was carried out by external chemical laboratories to characterize the material during maintenance and dredging activities in the reclamation channels. For this reason, not all concentrations of major and trace elements were available, but only those related to Annex IV of Legislative Decree 152/2006 were analyzed (D.Lgs n. 152/2006, 2006).

In March 2022, the database was integrated with 21 additional sediment samples (following Focus Area) collected where anomalous concentrations of PTEs and concentrations exceeding national regulation limits were spotted in the abovementioned LRC database, with particular attention also to areas with high salinity and low water table, that is, coastal pine forests (Cozzolino et al., 2017; Giambastiani et al., 2021). Sampling was performed using an auger at the bottom of the canals. For the geochemical characterization, sediment samples were oven-dried at 50°C for 24 hr, powdered, and homogenized in an agate mortar. The total concentration of major (SiO₂, TiO₂, Al₂O₃, Fe₂O₃, MnO, MgO, CaO, Na₂O, K₂O, P₂O₅, and LOI) and minor and trace elements (Al, As, Ba, Ca, Ce, Cl, Co, Cr, Cu, Fe, K, La, Mg, Mn, Na, Nb, Ni, P, Pb, Rb, Si, Sr, Th, Ti, V, Y, Zn, Zr) was determined by Wavelength Dispersive X-Ray Fluorescence (WDXRF) on pressed powder pellets using a Panalytical Axios 4000 spectrometer, following the methods proposed by Franzini et al. (1972) and Leoni and Saitta (1976) for matrix correction. The estimated precision and accuracy for trace-element determinations was 5%, except for those elements with low concentration (less than 10 ppm), for which the accuracy was lower (10%).

To account for differences in the analytical pools, and in the accuracy and data resolution resulting from the use of different analytical techniques (Poto et al., 2015), we chose to analyze and process the two data sets separately, both for geochemical characterization and statistical analysis.

To distinguish between localized enrichment in the canals and natural background concentrations, samples from the Focus Area were grouped based on their depositional facies (12 from BR; 7 from IF, 1 from CL, and 1 from SM, Figure 2). Then the total chemical compositions of these samples were compared to the results obtained by Buscaroli et al. (2021), who utilized the same analytical technique (WDXRF) to determine the total concentration of major and trace elements.

During the 2022 field campaign, at each sediment sampling point (Figure 2), drainage canal water was also collected using a bucket, and physical and chemical parameters (T, pH, EC) were measured in the field by using a multiparameter probe.

For the groundwater chemical characterization, four fully screened wells located along a 4 km long transect within the Focus Area (P2-5S; star symbols in Figure 2) were selected. Groundwater data, collected in previous studies by Greggio et al. (2020), were reprocessed here to obtain vertical profiles of physical parameters and chemical concentrations along the aquifer depth. As reported by Greggio et al. (2020), for each well, five groundwater samples were collected in November–December 2010 at different depths (i.e., at the water table, bottom, and corresponding to peat and fine-grained sediment layers) using straddle packers and following well purging procedures. Electrical conductivity (EC in mS/cm), temperature (T in °C), pH, and redox potential (Eh in mV) were measured in the field with a multiparameter device inserted in a flow cell to prevent rapid oxidation processes; major elements (SO_4^{2-} and HCO_3^-) were analyzed following the Italian National Environmental Agency standards (APAT-IRSA, 2003), while TEs (As, Fe, Mn) were analyzed by ICP-AES/ICP-MS (more details in Greggio et al., 2020).

3.2. Statistical Analysis

The statistical analysis was performed using PAST (Paleontological Statistics Software Package, v.4.11.; Hammer et al., 2001). The Mann-Whitney non-parametric test was performed to evaluate the statistical significance of the difference between the medians of sediment samples collected in the drainage canals of the Focus Area and soil samples collected by Buscaroli et al. (2021) in the same depositional environments. The significance correlations obtained were compared with <0.05 *p*-value.

Multivariate statistical analysis (PCA) was applied to two different scale data sets to investigate the complex multivariate relationship among variables and define a smaller number of Principal Components that can capture most of the variation between sediment samples. The first PCA was initially applied to the geochemical data of the sediment samples from the Focus Area (21 samples analyzed for the total content of major and trace elements by WDXRF; yellow dots in Figures 1 and 2) to deepen the hydrogeological and geochemical characterization of this coastal basin (Giambastiani et al., 2020; Greggio et al., 2020; Mollema et al., 2013, 2015; Soboyejo et al., 2021). Then a second PCA was performed on the geochemical data from the LRC sediment samples collected along the entire coastal area (182 samples analyzed by acid digestion and ICP-MS, red dots in Figures 1 and 2). Ideally, the phenomena revealed in the Focus Area based on a more extended analytical pool, would guide the PCA analysis and discussion performed for the entire coastal areas.

In both cases, PCA was performed on geochemical composition (mg/kg and %), along with several other physical variables of the sampling drainage canal, such as elevation (m a.s.l.), distance from the sea (km), and use of fertilizer in the surrounding land (kg/ha). The land elevation was provided by Lidar maps (1 × 1 m pixel); the distance from the sea was linearly calculated on GIS maps. In order to estimate the amount of fertilizers, the 2017 Corine Land Cover data set from the Emilia-Romagna geoportal (<https://geoportale.regione.emilia-romagna.it/>) was used and the specific crop types were extrapolated for the study area. The regional databases of technical standards of cultivation (<https://agricoltura.regione.emilia-romagna.it/produzioni-agroalimentari/temi/bio-agro-climambiente/fertilizzazione>) provided the standard amounts of fertilizer (N, P₂O₅, and K₂O in kg/ha) for each crop. If the sediment sample fell within an area dominated by a single crop, the total amount of fertilizers specified for that crop was assigned. However, if the sediment sample fell within an area with multiple crop types, an average value was used.

For the Focus Area, EC of the drainage water (mS/cm) and LOI of sediment samples (%) were also included in the PCA analysis.

4. Results

4.1. Geochemical Characterization

Table 1 shows the WDXRF results of the 21 sediment samples from the Focus Area (column A) along with the ICP-MS results of the LRC data set (column B). The entire data sets are reported in Tables S2 and S3 in Supporting Information S1.

For the 21 sediment samples collected in 2022 in the Focus Area, the abundance of major elements and LOI are ranked based on median concentrations and it is $\text{SiO}_2 > \text{LOI} > \text{CaO} > \text{Al}_2\text{O}_3 > \text{Fe}_2\text{O}_3 > \text{MgO} > \text{K}_2\text{O}$ with the following percentages: 44.9%, 16.7%, 14.4%, 10.2%, 4.9%, 3.6%, 1.9%, respectively. These sediment samples reveal a dominant sandy texture justified by high silica percentage, elevated amount of organic matter, and clay minerals.

Based on median concentrations, the minor and trace elements of the Focus Area sediment samples are ranked as follows: $\text{S} > \text{Sr} > \text{Ba} > \text{Cl} > \text{Crtot} > \text{Zr} > \text{Rb} > \text{V} > \text{Zn} > \text{Ni} > \text{Ce} > \text{Cu} > \text{Y} > \text{Pb} > \text{Co} > \text{Br} > \text{Nb} > \text{Th} > \text{As} > \text{Sn} > \text{Mo} = \text{U}$. Among the trace elements Cl has a range of concentration covering three orders of magnitude; As, Br, Co, Crtot, Cu, Nb, Pb and Sn cover two orders of magnitude, while Ba, Ce, Hg, Mo, Ni, Rb, S, Sr, Th, U, V, Zn, and Zr cover one order of magnitude. This testifies to the high variability of the substrate and the need for further research to investigate the source of the highest temporary concentrations. Moreover, As, Co, Cr, Cu, Pb, Sn, V, and Zn (almost all covering two orders of magnitude) exceed the legal Italian limits (Table S1 in Supporting Information S1), with 48% of the samples for Sn, 29% for V, and 24% for Crtot (bold in Table 1, part A). However, it is worth mentioning that the Italian legislation recommend aqua regia extraction, whereas for these samples WDXRF was adopted.

Among other variables included in the data set, EC ranges from 0.5 to 46 mS/cm, with a median value of 1.9 mS/cm. The drain bottoms range from -4.1 to 1 m a.s.l. with a median of -1.6 m a.s.l., reflecting the articulate network of canals, as well as depending on pumping station proximity. Samples were collected from the shoreline up to 18 km inland, with a median distance from the sea of 5 km. The impact of the agricultural activities is quantified proportional to the distribution of fertilizer per hectare, ranging from a minimum dose of 10 kg/ha (close to the natural area of coastal and historical pine forests) to a maximum dose of about 340 kg/ha in correspondence of fields cultivated with annual crops in the northwest of the Classe pine forest.

The LRC sediment analysis does not report major element concentrations and a shorter list of trace elements is available (Table 1, part B), consequently, no argument is made on their compositional and textural features. Based on median concentrations, the trace elements for the 182 LRC sediment samples are ranked as follows: $\text{Zn} > \text{Crtot} > \text{Ni} > \text{Cu} > \text{Pb} > \text{Co} > \text{As} > \text{Cd} > \text{Hg} > \text{Sn}$; maintaining the same order of abundance as samples of Focus Area. Cu, Pb, Sn, and Zn have a range of concentration covering two orders of magnitude, whereas As, Cd, Co, Crtot, Hg, and Ni cover one order of magnitude. Still, As, Cd, Cu, Pb, Sn, and Zn exceed Italian legal limits for 2%, 1%, 2%, 1%, 28%, and 6%, of the samples, respectively. Since samples are distributed over a larger portion of the coastal area, the median elevation of sampling is 0.8 m a.s.l., whereas distance from the sea and the average amount of applied fertilizer are still aligned to the Focus Area samples.

In order to evaluate natural and anthropogenic enrichments, sediment sample compositions of the Focus Area are compared with the near-surface sediments by Buscaroli et al. (2021), arranged based on the main depositional facies mapped in the area (BR and IF, Figure 2). Boxplots of sediment composition are shown in Figure 3. In the beach ridge deposits, As, Co and Fe concentrations are significantly higher in our samples than in the near-surface sediments collected by Buscaroli et al. (2021), whereas Co, Cu, Na and Sr appear to be significantly higher in both depositional facies: beach ridge and interfluvial floodplain deposits. For the other elements considered, there were no statistical enrichments and only Mn showed few outliers with high concentrations, well above the near-surface sediment values.

4.2. Focus Area

4.2.1. Principal Component Analysis

To understand the multivariate relationships between element concentrations and spatial variables in the Focus Area, the PCA of the 21 sediment samples was performed. Table 2 reports the component loadings for each

Table 1

Statistical Summary of the Sediment Compositions and PTEs Concentration in Samples Collected in 2022 (Columns A, 21 Samples From the Focus Area) and LRC Data set (Column B, 182 Samples; Refer to Figure 1 for Locations)

Sample	A							B						
	Min	Max	Mean	Median	Std dev.	Samples exceeding law limit for public, private, and residential green use (%)	Samples exceeding law limit for commercial and industrial use (%)	Min	Max	Mean	Median	Std dev.	Samples exceeding law limit for public, private, and residential green use (%)	Samples exceeding law limit for commercial and industrial use (%)
SiO ₂ (wt%)	26.7	52.9	43.7	44.9	6.9	#	#	#	#	#	#	#	#	#
TiO ₂ (wt%)	0.2	0.6	0.4	0.4	0.1	#	#	#	#	#	#	#	#	#
Al ₂ O ₃ (wt%)	2.6	13.5	9.3	10.2	2.9	#	#	#	#	#	#	#	#	#
Fe ₂ O ₃ (wt%)	2.2	35.2	7.0	4.9	7.4	#	#	#	#	#	#	#	#	#
MnO (wt%)	0.1	10.0	0.8	0.1	2.3	#	#	#	#	#	#	#	#	#
MgO (wt%)	2.2	4.2	3.4	3.6	0.7	#	#	#	#	#	#	#	#	#
CaO (wt%)	8.1	21.5	15.1	14.4	3.2	#	#	#	#	#	#	#	#	#
Na ₂ O (wt%)	0.5	4.1	1.2	0.8	1.0	#	#	#	#	#	#	#	#	#
K ₂ O (wt%)	0.3	2.6	1.9	1.9	0.5	#	#	#	#	#	#	#	#	#
P ₂ O ₅ (wt%)	0.1	0.4	0.2	0.2	0.1	#	#	#	#	#	#	#	#	#
LOI (%)	8.5	23.1	17.0	16.7	4.0	#	#	#	#	#	#	#	#	#
As (mg/kg)	3.0	108.0	12.9	6.0	22.5	9.5	4.8	0.0	57.0	5.4	5.0	5.5	1.7	0.6
Ba (mg/kg)	284.0	949.0	428.9	378.0	172.9	#	#	#	#	#	#	#	#	#
Br (mg/kg)	3.0	234.0	45.4	11.5	72.4	#	#	#	#	#	#	#	#	#
Ce (mg/kg)	10.0	76.0	44.0	46.0	16.5	#	#	#	#	#	#	#	#	#
Cl (mg/kg)	20.0	55660.0	5,574.8	280.0	14588.0	#	#	#	#	#	#	#	#	#
Cd (mg/kg)	#	#	#	#	#	#	#	0.03	10.0	0.3	0.2	0.8	0.6	0.0
Co (mg/kg)	4.0	126.0	19.1	14.0	25.6	14.3	0.0	0.0	18.5	7.9	8.5	4.7	0.0	0.
Cr _{tot} (mg/kg)	9.0	170.0	111.8	128.0	47.0	23.8	0.0	7.4	93.5	40.9	37.2	17.9	0.0	0.0
Cu (mg/kg)	6.0	195.0	48.7	39.0	41.4	9.5	0.0	2.0	290.0	37.8	31.4	29.6	2.2	0.0
Hg (mg/kg)	#	#	#	#	#	#	#	0.01	0.6	0.1	0.1	0.1	0.0	0.0
Mo (mg/kg)	<3	7.0	4.3	3.0	1.8	#	#	#	#	#	#	#	#	#
Nb (mg/kg)	5.0	14.0	10.6	11.0	2.6	#	#	#	#	#	#	#	#	#
Ni (mg/kg)	7.0	90.0	58.5	60.0	24.6	0.0	0.0	8.0	68.4	36.9	37.0	13.1	0.0	0.0
Pb (mg/kg)	3.0	185.0	24.3	16.0	37.1	4.8	0.0	1.0	537.0	19.0	14.0	41.4	1.1	0.0
Rb (mg/kg)	15.0	112.0	77.4	80.0	25.7	#	#	#	#	#	#	#	#	#
S (mg/kg)	210.0	5,510.0	1,792.4	1,420.0	1,498.3	#	#	#	#	#	#	#	#	#
Sn (mg/kg)	<3	10.0	5.2	4.0	2.1	47.6	0.0	0.0	100.0	1.2	0.0	7.5	27.5	0.0
Sr (mg/kg)	154.0	584.0	414.7	404.0	89.2	#	#	#	#	#	#	#	#	#
Th (mg/kg)	<3	24.0	8.8	7.0	4.5	#	#	#	#	#	#	#	#	#
U (mg/kg)	<3	4.0	3.2	3.0	0.4	#	#	#	#	#	#	#	#	#
V (mg/kg)	12.0	114.0	66.8	72.0	33.0	28.6	0.0	#	#	#	#	#	#	#
Y (mg/kg)	3.0	24.0	15.9	17.0	5.0	#	#	#	#	#	#	#	#	#
Zn (mg/kg)	20.0	188.0	79.9	66.0	46.4	9.5	0.0	0.0	569.9	71.9	69.2	64.3	5.5	0.0
Zr (mg/kg)	26.0	117.0	84.4	89.0	20.5	#	#	#	#	#	#	#	#	#

Table 1
Continued

Sample	A							B						
	Min	Max	Mean	Median	Std dev.	Samples exceeding law limit for public, private, and residential green use (%)	Samples exceeding law limit for commercial and industrial use (%)	Min	Max	Mean	Median	Std dev.	Samples exceeding law limit for public, private, and residential green use (%)	Samples exceeding law limit for commercial and industrial use (%)
Elevation (m a.s.l.)	-4.1	1.0	-1.5	-1.6	1.4	#	#	-2.8	13.5	2.0	0.8	3.6	#	#
Distance from the sea (km)	0.2	8.5	4.5	5.0	2.8	#	#	0.0	18.1	6.5	5.4	4.9	#	#
Fertilizer (kg/ha)	240.0	330.0	276.9	270.0	22.6	#	#	10.0	340.0	235.7	260.0	66.2	#	#
EC (mS/cm)	0.5	46.6	8.7	1.9	14.4	#	#	#	#	#	#	#	#	#

Note. Shown in bold are the concentrations of elements exceeding the D.Lgs n. 152/2006 law limits for public, private, and residential green uses and for commercial and industrial use (refer to Table S1 in Supporting Information S1 for soil contamination threshold limits); also reported are the percentages of samples exceeding these limits and summary of the physical variables used to perform PCA analysis (elevation, distance from the sea, and amount of fertilizer based on the Corine Land Cover classification). # denotes missing data or not applicable.

variable and statistical parameters used to evaluate the goodness-of-fit. Based on eigenvalues >1 , the selected 7 principal components explain 89.53% of the total variance.

The PC1 (Table 2) explains 48.05% of the variance with a marked bipartition among the variables. On one side K, Rb, Al, Y, Cr, Nb, Zr, V, Ti, Ni, Mg, and Zn have positive component loadings along with the distance from the sea. On the other side Na, Cl, Mo, Fe, As, Mn, Co, Br, S, and Ba have negative component loadings along with fertilizers and EC of the drainage water. When the scores of the PC1 are spatially located (Figure 4), the positive correlations are generally located in the inland plain deposits (CL and IF) and in correspondence with salt marsh and back ridge lagoon deposits (SM), even if five samples (n. 4, 11, 12, 14, and 15) with a small positive score (mean value of 1.4) are found in beach ridge facies associations (BR). The majority of negative correlations are in the BR facies, associated with coastal deposits, inner palaeodune belt, and quarry lakes (i.e., samples 16 and 22).

The PC2 (Table 2) explains 15.38% of the variance with evident bipartition. Co, V, Fe, Mg, Ni, Ce, Zn, As, and Ti have positive loadings, as well as fertilizers and LOI, whereas Sr, Si, and Ca show negative component loadings. The PC3 explains 8.33% of the variance. Ba, P, Br, S, and altimetry have positive correlations. The spatial distributions of PC2 and PC3 scores are shown in Figure S1 in Supporting Information S1. The positive PC2 scores are generally located in the finer deposits belonging to CL and IF facies associations, while the negative scores are in the BR deposits, apart from samples 2, 21, 11, and 15, which show opposite behavior.

4.2.2. EC and Fe + Mn Dependency

When drainage water EC is plotted against distance from the sea (Figure 5a), it is evident that the highest values of salinity (EC up to 46.6 mS/cm) are recorded within 2 km from the coast, drastically decreasing at greater distances. An exception is made for sample 8 due to the complexity of the drainage network in the pine forest, where water is drained toward the nearby pumping station located several kilometers inland.

Fe and Mn are the most reactive elements among the major constituents of the sediment and their sum (g/kg) is correlated with elements of PC1 having negative component loadings (the Pearson correlation values are listed in Table S4 in Supporting Information S1). The Fe + Mn concentrations correlate well with Cl, Co, and As (correlation values ≥ 0.85 , Figures 5b–5d). The binary plot of Fe + Mn and Cl concentrations (Figure 5b) reports good correlation ($R^2 = 0.96$) with samples 2, 3, and 21 showing simultaneous enrichment in Fe-Mn and saline water. Particularly evident is the correlation between Fe + Mn and As and Co where samples 2, 3, and 21 show the highest PTE concentrations. The linear dependency with As and Co is evident also at low Fe + Mn concentrations (Figures 5c and 5d). More binary plots of the PTEs concentrations versus Fe + Mn are shown in Figure S3 in Supporting Information S1.

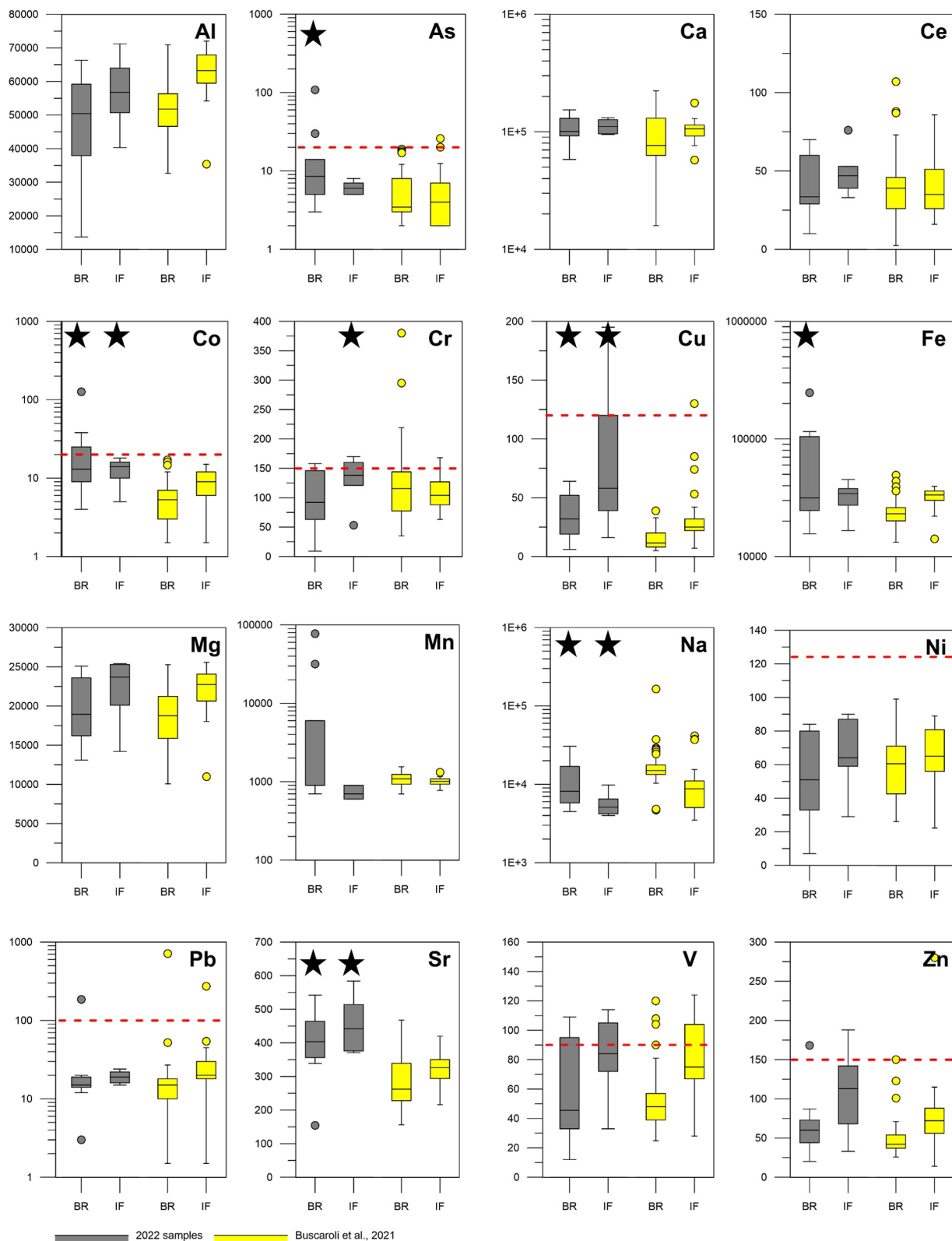


Figure 3.

4.2.3. Groundwater Geochemistry

Groundwater data from four wells located across the Focus Area are presented in Figure 6. Going westward, the pH rapidly increases, from values weakly acidic (around 6) in P2S to neutral values (7.5) in all other locations. The pH is vertically stable with uppermost values almost identical to those at the bottom of the aquifer. The EC groundwater data exceeds 40 mS/cm in P2S close to the shoreline, whereas brackish values are measured inland (ranging from 10 to 20 mS/cm, Figure 6a). The top water table has lower EC and higher redox potential than in the deep portion of the aquifer (Figure 6b), especially in wells located in the pine forest, where the aquifer is phreatic and directly recharged by rainfall (Greggio et al., 2020). In the deeper portion of the aquifer, there are anoxic conditions, and the redox potential ranges between -100 and -200 mV (Figure 6b).

In terms of element concentrations (Figure 6c), Fe is abundant in groundwater, with concentrations ranging between 0.3 and 13.5 mg/l. The concentration of Mn is on average 0.7 and 2.4 mg/l in P5S and P2S and decreases at 0.4–0.2 mg/l in P3S and P4S, respectively. The typical seawater sulfate concentration is present at P2S well and decreases moving inland. At the P4S location, sulfate is consumed because of the stronger anoxic conditions and concurrently increase in the production of bicarbonates at deeper levels. Groundwater from the deep portion of the coastal aquifer also shows enrichment in As with maximum values of 47.5 $\mu\text{g/l}$ in the most salinized and anoxic conditions (PS2); the concentration decreases by approximately 48% on average at the water table (Figure 6b).

4.3. LRC Sediment Samples

4.3.1. Principal Component Analysis

The results of the PCA performed on the 182 LRC samples are shown in Table 3.

The PC1 explains 27.2% of the variance with one positive component loading between Ni, Cr, Co, As, and fertilizers. Once the scores of the PC1 are spatially located (Figure S2a in Supporting Information S1), the positive values are well grouped and located in the southern part of the studied coastal area, whereas samples to the north show negative scores with only sporadic positive scores.

The PC2 explains 16.69% of the variance with a marked bipartition among variables: Cu, Zn, and Pb, along with Cr and Ni have positive correlations, whereas As, Co, Sn, and fertilizers have negative correlations. It is interesting to note that, as for the Focus Area, even here the group As, Co, and fertilizers show an opposite behavior compared to Cu, Zn, Pb, Cr, and Ni groups. The Cu, Zn, and Pb of PC2 have the highest scores close to the anthropic settlements (Figure S2b in Supporting Information S1). The PC3 accounts for 13.23% of the variance and it is guided by Sn, Pb, and As elements. The higher scores are in a few samples, especially concentrated close to industrial harbor areas in the northeast of Ravenna.

5. Discussion

The sediment samples in the Focus Area revealed a primarily sandy texture with a clear Ca-dominant signal (Table 1A) for the Holocene beach ridge deposits (BR), which are largely of Apennine provenance (Greggio, Giambastiani, & Antonellini, 2018; Greggio, Giambastiani, Campo, et al., 2018). Based on Buscaroli et al. (2021), geochemical differences would be expected among samples from BR and fine-grained interfluvial floodplain depositional facies (IF), which are mainly characterized by high abundance of Al_2O_3 , K_2O , LOI, along with high trace elements (Co, Cu, Rb, V, Zn) concentrations due to their affinity with clay minerals. However, the geochemical homogeneity observed in sediment composition within the drains suggests that fine-grained particles are preferentially eroded from the surrounding cultivated soils during intense rainfall events, and then transported and deposited within the canals leading to an increase in the finer composition of the original bed sediments. Although in flat agricultural areas, the rainfall-induced soil erosion is limited compared to hill shaded areas (i.e., Piacentini et al. (2018) report 30 mm/day of erosion), it does occur and leads to a sorting of finer grains on the

Figure 3. Sediment compositions (mg/kg) of samples collected in 2022 along the drainage ditches of the Focus Area (gray boxplots) compared to the results of Buscaroli et al. (2021) (yellow boxplots). Boxplots of elements are arranged based on the depositional facies mapped in the area: BR = beach ridge deposits; IF = interfluvial floodplain deposits (refer to Figure 2). Note: SM (salt marsh and back ridge lagoon) and CL (channel, levee, and river flooding) deposits are not shown because of lack of representative number of samples (1 for SM and 1 for CL). Red dashed lines indicate threshold limits of the Italian environmental law (D.Lgs n. 152/2006, 2006). The star symbols indicate elements for which the statistical median difference calculated by the Whitney non-parametric test between Buscaroli et al. (2021) and 2022 Focus Area samples is significant at <0.05 p -value. Graphs of As, Ca, Co, Fe, Mn, Na, and Pb have logarithmic y -axis to enhance the visualization of data distribution.

Table 2
Component Loadings of Each Variable for the Focus Area Samples; Eigenvalues, Explained % of Variance, and Cumulative % of Variance for Each Selected Component (PC1–PC7)

Variables	Component loadings						
	PC 1	PC 2	PC 3	PC 4	PC 5	PC 6	PC 7
Si	0.56	-0.74	-0.27	-0.01	-0.14	-0.07	0.11
Ti	0.82	0.44	0.02	0.08	-0.13	-0.10	-0.01
Al	0.93	0.08	0.07	0.09	-0.04	-0.20	0.05
Fe	-0.81	0.52	-0.12	0.00	0.02	-0.18	0.06
Mn	-0.74	0.28	0.21	0.30	0.14	0.36	-0.23
Mg	0.72	0.51	0.12	0.13	0.03	0.07	-0.10
Ca	0.22	-0.87	0.30	0.04	0.16	-0.17	0.00
Na	-0.96	0.05	0.10	0.18	0.02	0.07	-0.06
K	0.96	0.10	-0.05	0.05	-0.06	0.11	-0.09
P	-0.05	0.17	0.74	0.06	-0.06	-0.54	0.25
As	-0.80	0.41	-0.31	-0.06	0.13	-0.21	0.10
Br	-0.69	0.24	0.40	0.10	-0.38	0.22	-0.04
LOI	0.04	0.57	0.37	-0.27	0.02	0.35	-0.13
Ba	-0.48	0.06	0.57	0.44	-0.05	-0.12	0.02
Ce	0.72	0.47	-0.31	0.11	-0.13	-0.08	0.25
Cl	-0.90	0.38	-0.05	0.12	0.13	-0.01	-0.04
Co	-0.73	0.55	-0.26	-0.05	0.11	-0.25	0.07
Cr	0.91	0.36	0.03	-0.02	-0.09	-0.03	-0.06
Cu	0.44	0.25	0.49	-0.34	0.38	-0.11	0.21
Mo	-0.90	0.36	0.10	0.15	0.02	0.07	-0.05
Nb	0.88	0.39	0.01	0.13	-0.07	0.07	0.01
Ni	0.77	0.50	0.03	0.03	-0.20	0.13	-0.12
Pb	0.11	-0.11	-0.20	0.15	-0.06	0.48	0.80
Rb	0.94	0.25	-0.09	-0.02	-0.08	0.10	-0.04
S	-0.52	0.11	0.54	-0.34	-0.09	0.03	0.14
Sn	0.05	0.09	0.32	-0.21	-0.78	-0.12	-0.04
Sr	0.45	-0.42	0.49	-0.09	0.36	0.32	-0.08
Th	-0.48	0.64	-0.27	0.09	0.36	-0.08	0.11
U	0.32	0.22	-0.21	0.64	-0.02	-0.24	-0.13
V	0.83	0.54	-0.01	0.01	-0.05	0.04	-0.05
Y	0.92	0.20	0.07	0.23	0.13	0.04	-0.02
Zn	0.59	0.45	0.45	-0.17	0.29	-0.08	0.19
Zr	0.84	-0.08	0.16	0.32	0.19	0.02	0.00
EC	-0.80	-0.12	0.13	0.27	0.03	0.02	-0.16
Distance from the sea (km)	0.71	0.17	-0.11	-0.25	0.34	0.01	-0.22
Altimetry (m a.s.l.)	0.20	-0.19	0.26	0.87	0.04	0.08	0.15
Land Use fertilizers (kg/ha)	-0.65	0.49	-0.04	-0.06	-0.11	0.28	0.16
Eigenvalue	17.78	5.69	3.07	2.33	1.67	1.42	1.18
% variance	48.05	15.38	8.29	6.29	4.51	3.84	3.18
Cum. % variance	48.05	63.43	71.71	78.00	82.51	86.35	89.53

Note. In the table, normal bold entries = positive correlation >0.5; italic bold entries = negative correlation <-0.5; ascending red and blue color scales indicate ascending positive and negative component loading values, respectively.

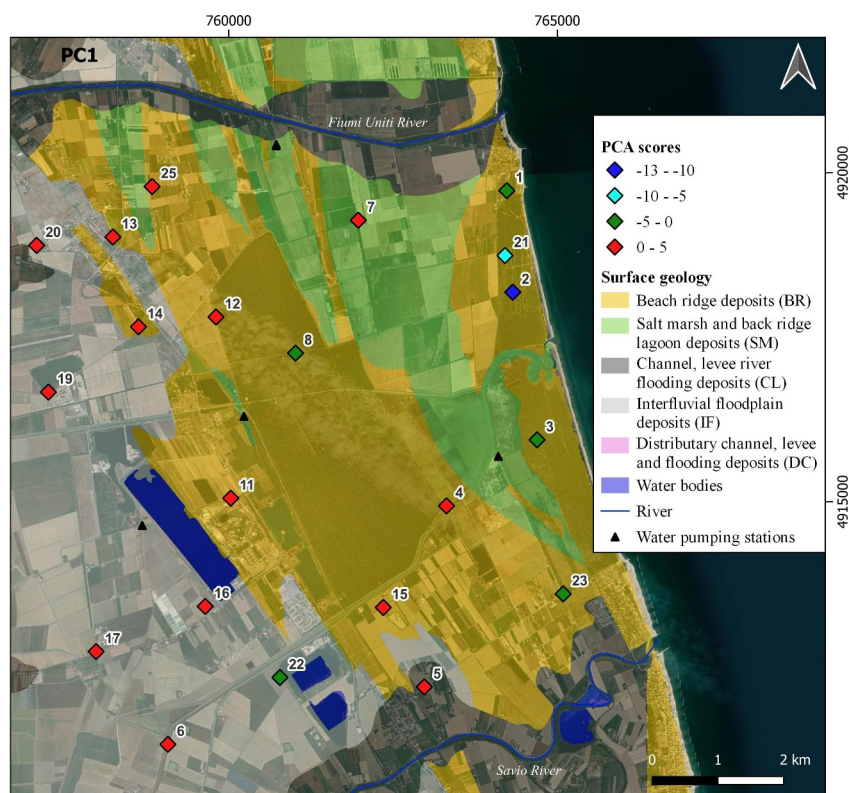


Figure 4. Scores distribution of PC1 components in the Focus Area.

drain beds compared to the associated depositional facies. Despite this, the comparison of these drainage canal sediments with near-surface sediments by Buscaroli et al. (2021) confirms the enrichment of some elements in these locations. As shown in Figure 3, the statistically significant enrichments of As, Co, Cr, Cu, Fe, and Sr (including some outliers like Mn) suggest that the interaction between sediment and drainage water alters the sediment trace element compositions. These enrichments in PTEs are significant for samples collected from both BR and IF facies.

The drainage water EC values (Table 1) show the presence of brackish-saline water in the canals. As reported in other studies carried out in the area (Cozzolino et al., 2017; Giambastiani et al., 2021), there is a general decreasing salinity gradient toward inland areas, and the closer the drains to the coastline, the higher the EC values of the drainage water (i.e., 44–33 mS/cm in Samples 1 and 2, respectively, Table S2 in Supporting Information S1 and Figure 5). In this context, along with the low topography and shallow water table areas, another major driver of soil and water salinization is the drainage network that causes an upward seepage of saline water from the bottom of the salinized coastal aquifer (Giambastiani et al., 2018, 2020; Soboyejo et al., 2021).

The PCA results for the Focus Area show that in PC1 (Table 2 and Figure 4) Na, Cl, Mo, Fe, As, Mn, Co, Br, S, and Ba have negative correlations with the use of fertilizers and drainage water EC. It must be noted that this group of elements with negative component loadings contains the same elements (As, Co, Fe, Mn) that are statistically enriched compared to background composition (Buscaroli et al., 2021); this indicates the presence of interaction processes between surface and groundwater that result in the enrichment of PTEs in the drainage system, as explained below. Na, Cl, Br, and S have clear marine origin, confirming the presence of saline groundwater in the drains and influence of seawater seepage as the main source of these elements, especially along the coastline and in the drainage network of the coastal pine forests (Figure 4).

The drainage water reflects the groundwater composition of the underlying salinized coastal aquifer that is characterized by high salinity values (up to 25.5 g/l, Cozzolino et al., 2017; Figure 6a), strong negative redox potential (Marconi et al., 2011; Figure 6b), neutral pH (Figure 6a), high alkalinity (Figure 6c), and enrichment in As and Fe (among other elements; Mollema et al., 2015; Figures 6b and 6c, respectively) due to the anaerobic

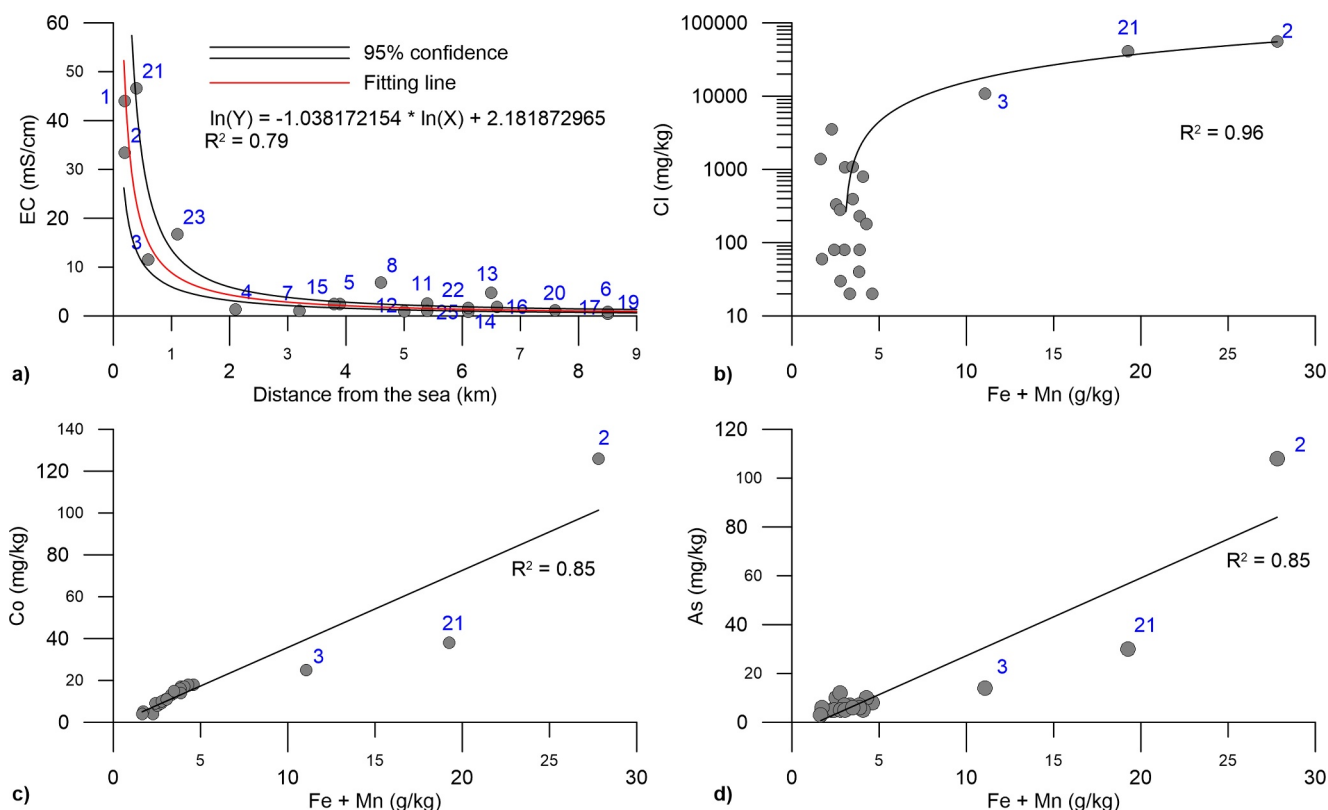


Figure 5. Binary plots of the Focus Area sediment samples: (a) drainage water EC versus distance from the sea; (b) Cl versus Fe + Mn; (c) Co versus Fe + Mn; (d) As versus Fe + Mn. Note: graph in (b) has logarithmic y-axis to enhance the visualization of data distribution.

degradation of abundant organic matter within the aquifer (Filippini et al., 2021; Giambastiani et al., 2013; Mollema et al., 2013). The mobility and occurrence of As in groundwater is strongly dependent on its oxidation state. The reduced form of As (As^{3+}) has greater mobility, while the oxidized form (As^{5+}) tends to be absorbed by Fe-, Al-, and Mn- hydroxides, clay minerals, and organic matter, favoring precipitation and removal from solution. The reductive dissolution of Fe- and Mn- oxides and hydroxides (HFO, HMO from now on), which is linked to the anaerobic degradation of peat layers, has been identified as the main As source from sediment to groundwater (Carraro et al., 2015; Colombani et al., 2015; Guo et al., 2011; Mollema et al., 2013; Rotiroti et al., 2015). In this context, salinity plays a critical role due to the presence of high concentration of SO_4^{2-} that can be used by sulfate-reducing bacteria as terminal electron acceptors during the anaerobic decomposition of OM in a reducing aquifer (Hackney & Avery, 2015). Once the oxygen-poor saline groundwater with high concentrations of Fe, Mn, As, and other elements, such as Mo, Co, Zn, etc. (Greggio et al., 2020) reaches the drainage canals, the mixing with meteoric water increases the redox potential into positive values and causes the formation and precipitation of HFO and HMO. High concentrations of HFO and HMO are found in the sediments (Table 1 and Figure 3) as also testified by the reddish color of water and sludge in the drains, especially in high salinity conditions (Figures 5a and 5b). The precipitation of HFO and HMO results in the removal of dissolved trace elements from the solution and their transfer into the solid phase (Manceau et al., 1992; Mollema et al., 2015; Ravenscroft et al., 2009; Stockdale et al., 2010; Weiske et al., 2013). This process explains the concurrent high concentrations of Fe_2O_3 , MnO, As, Co, Mo, and other PTEs, with the most saline samples (2, 3, and 21) dominating the correlation (Figures 5c and 5d and Figure S3g in Supporting Information S1). A Sequential Extraction Procedure (SEP) would be necessary to gain more information on contaminant pools with differential lability of As and other PTEs in various solid phases. This procedure would also indicate the potential effects of changing conditions (i.e., oxic and anoxic) within the system (Toller et al., 2022; Wenzel et al., 2001). In the present study, these techniques are not employed due to the large number of samples but also because the results would not be easily compared with the pseudo-total results of the LCR samples obtained by aqua regia digestion.

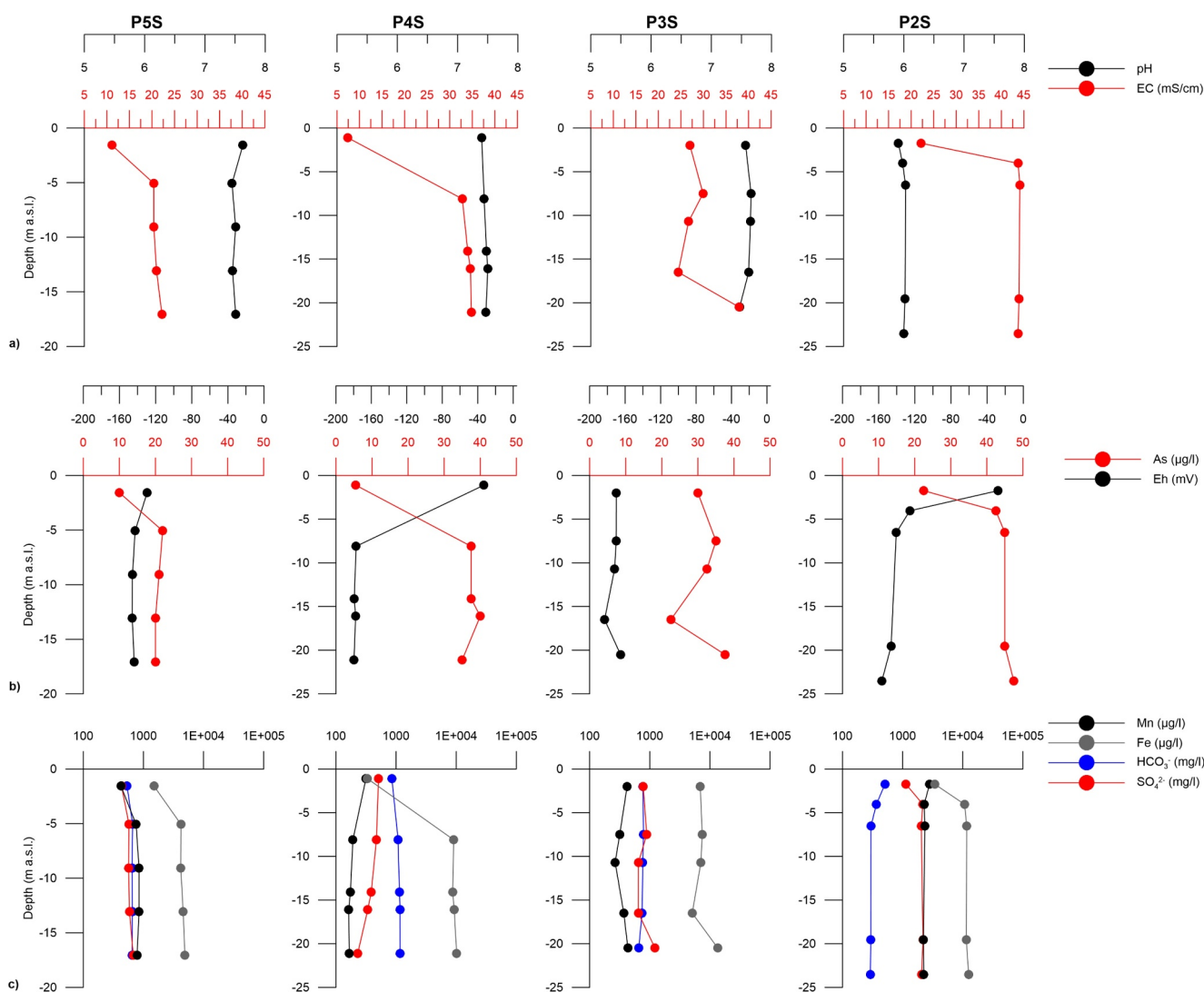


Figure 6. Vertical distribution of physical and chemical groundwater parameters in the Focus Area. Refer to Figure 2 for the well locations.

The PC1 on the Focus Area samples (Table 2) groups together many elements with positive loadings, such as K, Rb, Al, Y, Cr, Nb, Zr, V, Ti, Ni, Mg, and Zn along with the distance from the sea. As confirmed by Dinelli et al. (2007) and Buscaroli et al. (2021), these elements are positively correlated with silty clay and clay sediments that characterized the inland portion of the study area, where the phreatic aquifer becomes semi-confined due to the alluvial plain deposits and back barrier facies association (Amorosi et al., 2008) (Figure 2). The dependency with the distance from the sea confirms the chemical distribution (Figure 4); as suggested by Du Laing et al. (2008) high EC values promote Cr, Ni and Zn desorption from the sediment, which result in decreasing concentrations in sediments and increasing concentrations in water.

Extending the analysis to the entire coastal area, PC1 results in Table 3 show positive correlation between Ni, Cr, Co, and As, along with the use of fertilizers. Their location in the southern part of the area (Figure S2a in Supporting Information S1) agrees with the natural background concentration map of Cr developed by the Emilia Romagna Region (https://ambiente.regione.emilia-romagna.it/en/geologia/soil/heavy-metals-in-soil/pedogeochemical-ER-plain?set_language=en) that identifies natural enrichments of Cr in the inland portion of the plain westward of the city of Cervia, corresponding to IF depositional facies. Indeed, silty clay deposits are naturally enriched in Ni, Cr, and Co as highlighted by Dinelli et al. (2007). The correlation between this group of elements and the use of fertilizers is reasonable since the southern coast is entirely occupied by tourist infrastructure, while agricultural activities is dominant in the inner regions. The agricultural activities and the current drainage management of the

Table 3
LRC Samples Component Loadings for Each Variable; Eigenvalues, Explained % of the Variance, and Cumulative % of the Variance for Each Selected Component (PC1–PC4)

Variables	PC 1	PC 2	PC 3	PC 4
As (mg/kg)	0.50	−0.36	0.52	−0.02
Co (mg/kg)	0.76	−0.23	−0.24	0.10
Cr (mg/kg)	0.80	0.37	−0.25	−0.08
Ni (mg/kg)	0.88	0.25	−0.23	−0.04
Pb (mg/kg)	0.00	0.42	0.43	−0.18
Cu (mg/kg)	0.06	0.77	0.05	0.17
Zn (mg/kg)	0.08	0.61	0.42	−0.02
Sn (mg/kg)	0.13	−0.14	0.65	0.13
Distance from the sea (km)	−0.15	0.13	−0.08	0.94
Land Use fertilizers (kg/ha)	0.64	−0.33	0.30	0.24
Eigenvalue	2.72	1.67	1.32	1.04
% variance	27.20	16.69	13.23	10.39
Cum. % variance	27.20	43.89	57.12	67.50

Note. In the table, normal bold entries = positive correlation >0.5; italic bold entries = negative correlation <−0.5; ascending red and blue color scales indicate ascending positive and negative component loading values, respectively.

area probably contribute to the distribution and accumulation of PTEs in drain bed sediments. Moreover, the complex drainage system that controls the water table in the study area can be a pathway for the transport of fertilizers and other agricultural chemicals into drainage water (Mastrocicco et al., 2012, 2013, 2016). The concentration of PTEs, such as As, Cd, Cr, Pb, Hg, and Ni in fertilizers, as impurities or contaminants, can vary depending on the source and type of fertilizer (Gharaibeh et al., 2020; Sacchi et al., 2020; Weissengruber et al., 2018). Where fertilizers are applied to crops, dissolved elements can be carried away by rainfall or irrigation water, and ultimately end up in the drainage system and here undergo water-sediment interactions. It has to be noted that crop rotation practices could hinder the statistical validity of this parameter in the PCA analysis because the application of fertilizers may vary over time in response to changes in crops and agricultural practices.

The PC2 results for the entire coastal area (Table 3) show high correlation among Cu, Zn, and Pb, followed by Cr and Ni, although with lower values. Several works recognize Cu, Pb, Zn, and Cr as elements related to road traffic and transportation and, generally, as anthropogenic tracers (Budai & Clement, 2018; Świetlik et al., 2015). Cu, Pb, and Zn loads, which are released from brake and tire wear, can be easily mobilized during rainfall, along with the fine particles they are associated with. These elements can then return to the atmosphere through resuspension when the roadside dust dries up (Budai & Clement, 2018). These processes control the mobility of these elements in the air and drainage water outside the road areas, and may explain the enrichments observed in samples located near major roads or industrial facilities (Figure S2b in Supporting Information S1), even if no significant trends are discernible.

Although it is well-established that hydrous Mn oxides have strong affinity for adsorbing Pb^{2+} across a wide range of pH values (Covelo et al., 2007; Manceau et al., 1992), we observe an exception in the case of sample 4 (Figure S3a in Supporting Information S1). This sample, which contains the highest concentration of Pb (158 mg/kg) and relatively low content of Fe and Mn oxides, was collected from an irrigation canal bordering a wetland historically used for waterfowl hunting. The elevated Pb concentration may be attributed to the wide dispersal of lead pellets in such wetland areas as discussed in Migani et al. (2015).

Chromium, in its reduced state, has a strong affinity for HFO and HMO, but reaction products are different (Manceau et al., 1992): HFO fixes it (with possible transport in particulate form), whereas HMO oxidizes and then solubilizes it (Richard & Bourg, 1991). The high affinity of Cr for HFO results in the formation of widespread Cr-containing Fe oxides. At a molecular level, the trapping of Cr^{3+} by HFO is achieved either through the formation of surface complexes on already formed Fe particles (as in an adsorption/surface precipitation phenomenon), or through the simultaneous hydrolysis of Fe^{3+} and Cr^{3+} (as in a co-precipitation phenomenon). In this case study, Cr concentration is low where Fe and Mn oxides have high values (Figure S3c in Supporting Information S1) as in the three samples of the pine forest (2, 3, 21). This can be explained by the high salinity that increases PTE mobilization in soils and reduces the sorption capacities of Fe- and Mn-oxides. The extent of mobilization depends on the type and total amount of PTEs, as well as the type of salt causing the salinization (Acosta et al., 2011; Choi et al., 2020; Du Laing et al., 2008). In particular, the major mechanisms affecting the salinization process are the complexation capacity of salt derived anions with PTEs, and competition of salt derived cations with positively charged PTEs for sorption sites on the solid phase (Acosta et al., 2011; Paalman et al., 1994).

According to Gadde and Laitinen (1974), Zn, which is present in many fertilizers, is also adsorbed on HFO and HMO at high pH (>7). In Figure S3b in Supporting Information S1, Zn concentration increases with increasing $Fe_2O_3 + MnO$ % in most samples, except once again, for the saline samples collected in the coastal pine forests.

Tin (Sn) shows the major % exceeding the national threshold in Table 1. Tin is a poorly studied element in soil and sediment and its average value in soil is 1.1 mg/kg (Salminen et al., 2005). Anthropogenic sources of Sn are coal and wood combustion, waste incineration and sewage sludge, solder (Sn-Pb), agricultural

pesticides, and wood preservatives with organo-Sn compounds (Reimann & De Caritat, 1998). In water, Sn^{2+} is rapidly oxidized and is subsequently bound to secondary oxides of Fe or Al as $\text{Sn}(\text{OH})_4$ or $\text{Sn}(\text{OH})_3\text{O}^-$ with affinity for the finest particulate matter. Here, Sn does not show a correlation with Fe and Mn (Figure S3f in Supporting Information S1), and the highest concentrations are located along the main roads and railways. Indeed, a recent work by Stančić et al. (2022) indicated railway-originated dust as a potential source of Sn in nearby soil.

6. Conclusions

This study addresses a gap in the scientific literature concerning the distribution and accumulation of various Potentially Toxic Elements (PTEs) in sediments from drainage canals in low-lying coastal reclamation areas. The aim of the study is to obtain evidence of the geochemical processes occurring between drainage water and canal bed sediments and assess the factors affecting PTEs distribution and enrichment.

The sediment samples reveal high concentrations of PTEs, exceeding the limits set by the Italian Environmental Law. A comparison with near-surface sediment samples shows significant enrichment of As, Co, Cr, Cu, Fe, Na, and Sr, and the results of the multivariate statistical analysis (PCA) indicate the drainage water salinity, topography, and fertilizer usage as the main causes.

Strong positive correlations between As, Co, Mo, and iron and manganese oxides suggest that the absorption on Fe- and Mn oxyhydroxides (HFO and HMO) is the primary mechanism for PTE precipitation from the solution and enrichment in the sediments, especially in areas with high salinity conditions near the sea (e.g., coastal pine forests). The drainage causes seepage of saline, anoxic, and Fe- and Mn-enriched groundwater from the bottom of the salinized coastal aquifer; the mixing with meteoric water increases the redox potential causing the formation and precipitation of HFO and HMO that remove the dissolved trace elements from the solution into solid phase. Among the PTEs, Cr and Ni abundances are explained by natural background values and, locally, by fertilizer application, while enrichments of Cu, Pb, and Zn are recognized as anthropic tracers and are associated with proximity to main roads. However, under conditions of high electrical conductivity, these PTEs preferentially remain in solution due to competition with salt-derived cations for sites in solid phases.

Since drainage canals are regularly dredged to maintain the required hydraulic gradient, it is essential to characterize the geochemical composition of the sediment to determine if it can be reused or disposed of safely. High concentrations of PTEs in the sludge and sediments classify them as special wastes, necessitating costly protocols and procedures for treatment and disposal. Moreover, understanding the fate and mobility of heavy metals between water and sediment matrix is crucial due to the use of these channels for irrigation during the spring-summer season.

The study area (Ravenna, Po river delta plain, Italy) serves as a representative case study for the complex issues that many low sandy coasts and delta regions face worldwide. The interplay of water and soil salinization, subsidence, land reclamation, coastal urbanization, and climate change, including sea level rise and extreme events, will intensify the geochemical processes outlined in this paper. These heightened interactions will make coastal areas more vulnerable to sediment toxicity, particularly in the event of mismanagement, such as improper agricultural practices, human activities contributing to land subsidence, or extensive drainage. The insights gained from this research can provide valuable information to water management institutions worldwide, assisting them in making informed decisions and implementing effective strategies to manage dredged sediments and address the challenges associated with the presence of PTEs in the reclaimed coastal areas, and ensure their long-term resilience.

Lastly, to control further enrichment and accumulation of PTEs in canal sediments, the water management institutions should establish a monitoring network to periodically check the use of fertilizers and the Eh-pH-salinity conditions, as these factors play fundamental roles in the mobility of PTEs.

Data Availability Statement

Data sets related to this article can be found at Giambastiani et al. (2023) [Dataset], in the open-source online data repository hosted at Zenodo.

Acknowledgments

The authors would like to thank the Land Reclamation Consortium (Consorzio di Bonifica della Romagna, Ravenna, Italy) for making available the drainage data and part of the sediment analysis.

References

- Abdelrady, A., Bachwenkizi, J., Sharma, S., Sefelnasr, A., & Kennedy, M. (2020). The fate of heavy metals during bank filtration: Effect of dissolved organic matter. *Journal of Water Process Engineering*, 38, 101563. <https://doi.org/10.1016/j.jwpe.2020.101563>
- Abdu, N., Abdullahi, A. A., & Abdulkadir, A. (2017). Heavy metals and soil microbes. *Environmental Chemistry Letters*, 15(1), 65–84. <https://doi.org/10.1007/s10311-016-0587-x>
- Acosta, J. A., Jansen, B., Kalbitz, K., Faz, A., & Martínez-Martínez, S. (2011). Salinity increases mobility of heavy metals in soils. *Chemosphere*, 85(8), 1318–1324. <https://doi.org/10.1016/j.chemosphere.2011.07.046>
- Adriano, D. C. (2001). Trace elements in terrestrial environments biogeochemistry, bioavailability, and risks of metals (II ed.).
- Adriano, D. C., Wenzel, W. W., Vangronsveld, J., & Bolan, N. S. (2004). Role of assisted natural remediation in environmental cleanup. *Geoderma*, 122(2–4), 121–142. <https://doi.org/10.1016/j.geoderma.2004.01.003>
- Ahado, S. K., Nwaogu, C., Sarkodie, V. Y. O., & Borůvka, L. (2021). Modeling and assessing the spatial and vertical distributions of Potentially Toxic Elements in soil and how concentrations differ. *Toxics*, 9(8), 181. <https://doi.org/10.3390/toxics9080181>
- Ahmad, N., Usman, M., Ahmad, H. R., Sabir, M., Farooqi, Z. R., & Shehzad, M. T. (2023). Environmental implications of phosphate-based fertilizer industrial waste and its management practices. *Environmental Monitoring and Assessment*, 195(11), 1326. <https://doi.org/10.1007/s10661-023-11958-4>
- Amorosi, A., Dinelli, E., Rossi, V., Vaiani, S. C., & Sacchetto, M. (2008). Late Quaternary palaeoenvironmental evolution of the Adriatic coastal plain and the onset of Po River Delta. *Palaeogeography, Palaeoclimatology, Palaeoecology*, 268(1–2), 80–90. <https://doi.org/10.1016/j.palaeo.2008.07.009>
- Amorosi, A., & Sammartino, I. (2007). Influence of sediment provenance on background values of potentially toxic metals from near-surface sediments of Po coastal plain (Italy). *International Journal of Earth Sciences*, 96(2), 389–396. <https://doi.org/10.1007/s00531-006-0104-8>
- Amorosi, Colalongo, Pasini, & Preti (1999). Sedimentary response to Late Quaternary sea-level changes in the Romagna coastal plain (northern Italy). *Sedimentology*, 46(1), 99–121. <https://doi.org/10.1046/j.1365-3091.1999.00205.x>
- Antonellini, M., Giambastiani, B. M. S., Greggio, N., Bonzi, L., Calabrese, L., Luciani, P., et al. (2019). Processes governing natural land subsidence in the shallow coastal aquifer of the Ravenna coast, Italy. *Catena*, 172, 76–86. <https://doi.org/10.1016/j.catena.2018.08.019>
- Antonellini, M., Mollema, P., Giambastiani, B., Bishop, K., Caruso, L., Minchio, A., et al. (2008). Salt water intrusion in the coastal aquifer of the southern Po Plain, Italy. *Hydrogeology Journal*, 16(8), 1541–1556. <https://doi.org/10.1007/s10040-008-0319-9>
- APAT-IRSA. (2003). *Metodi analitici per le acque – Volume Primo. Agenzia per la Protezione dell'ambiente e per i servizi tecnici*. Istituto di Ricerca sulle Acque. Retrieved from https://www.irsna.cnr.it/wp/wp-content/uploads/2022/04/Vol1_Sez_1000_Indice_ParteGenerale.pdf
- Appelo, C. A. J., & Postma, D. (2004). In C. A. J. Appelo & D. Postma (Eds.), *Geochemistry, groundwater and pollution*. CRC Press. <https://doi.org/10.1201/9781439833544>
- Asati, A., Pichhode, M., & Nikhil, K. (2016). Effect of heavy metals on plants: An overview. *International Journal of Application or Innovation in Engineering & Management (IJAIEM)*, 5(3), 56–66.
- Balali-Mood, M., Naseri, K., Tahergorabi, Z., Khazdair, M. R., & Sadeghi, M. (2021). Toxic mechanisms of five heavy metals: Mercury, lead, chromium, cadmium, and arsenic. *Frontiers in Pharmacology*, 12, 643972. <https://doi.org/10.3389/fphar.2021.643972>
- Benini, L., Antonellini, M., Laghi, M., & Mollema, P. N. (2016). Assessment of water resources availability and groundwater salinization in future climate and land use change scenarios: A case study from a Coastal Drainage Basin in Italy. *Water Resources Management*, 30(2), 731–745. <https://doi.org/10.1007/s11269-015-1187-4>
- Bernhoft, R. A. (2012). Mercury toxicity and treatment: A review of the literature. *Journal of Environmental and Public Health*, 2012, 1–10. <https://doi.org/10.1155/2012/460508>
- Bianchini, A., Cento, F., Guzzini, A., Pellegrini, M., & Saccani, C. (2019). Sediment management in coastal infrastructures: Techno-economic and environmental impact assessment of alternative technologies to dredging. *Journal of Environmental Management*, 248, 109332. <https://doi.org/10.1016/j.jenvman.2019.109332>
- Bijlsma, M., Galione, A. L. S., Kelderman, G., Alaerts, G. J., & Clarisse, I. A. (1996). Assessment of heavy metal pollution in inner-city canal sediments. *Water Science and Technology*, 33(6), 231–237. <https://doi.org/10.2166/wst.1996.0101>
- Budai, P., & Clement, A. (2018). Spatial distribution patterns of four traffic-emitted heavy metals in urban road dust and the resuspension of brake-emitted particles: Findings of a field study. *Transportation Research Part D: Transport and Environment*, 62, 179–185. <https://doi.org/10.1016/j.trd.2018.02.014>
- Buscaroli, A., Gherardi, M., Vianello, G., Vittori Antisari, L., & Zannoni, D. (2009). Soil survey and classification in a complex territorial system: Ravenna (Italy). *EQA – Envir. Qual.*, 2, 15–28. <https://doi.org/10.6092/issn.2281-4485/3815>
- Buscaroli, A., Zannoni, D., & Dinelli, E. (2021). Spatial distribution of elements in near surface sediments as a consequence of sediment origin and anthropogenic activities in a coastal area in northern Italy. *Catena*, 196, 104842. <https://doi.org/10.1016/j.catena.2020.104842>
- Campo, B., Amorosi, A., & Vaiani, S. C. (2017). Sequence stratigraphy and late Quaternary paleoenvironmental evolution of the Northern Adriatic coastal plain (Italy). *Palaeogeography, Palaeoclimatology, Palaeoecology*, 466, 265–278. <https://doi.org/10.1016/j.palaeo.2016.11.016>
- Carraro, A., Fabbri, P., Giaretta, A., Peruzzo, L., Tateo, F., & Tellini, F. (2015). Effects of redox conditions on the control of arsenic mobility in shallow Alluvial Aquifers on the Venetian Plain (Italy). *Science of the Total Environment*, 532, 581–594. <https://doi.org/10.1016/j.scitotenv.2015.06.003>
- Choi, J., Septian, A., & Shin, W. S. (2020). The influence of salinity on the removal of Ni and Zn by sorption onto iron oxide- and manganese oxide-coated sand. *Sustainability*, 12(14), 5815. <https://doi.org/10.3390/su12145815>
- Colombani, N., Mastrociccio, M., & Dinelli, E. (2015). Trace elements mobility in a saline coastal aquifer of the Po river lowland (Italy). *Journal of Geochemical Exploration*, 159, 317–328. <https://doi.org/10.1016/j.gexplo.2015.10.009>
- Cook, S. R., & Parker, A. (2003). Geochemical changes to dredged canal sediments following land spreading: A review. *Land Contamination and Reclamation*, 11(4), 405–410. <https://doi.org/10.2462/09670513.627>
- Covelo, E. F., Vega, F. A., & Andrade, M. L. (2007). Competitive sorption and desorption of heavy metals by individual soil components. *Journal of Hazardous Materials*, 140(1–2), 308–315. <https://doi.org/10.1016/j.jhazmat.2006.09.018>
- Cozzolino, D., Greggio, N., Antonellini, M., & Giambastiani, B. M. S. (2017). Natural and anthropogenic factors affecting freshwater lenses in coastal dunes of the Adriatic coast. *Journal of Hydrology*, 551, 804–818. <https://doi.org/10.1016/j.jhydrol.2017.04.039>
- Di Giuseppe, D., Faccini, B., Mastrociccio, M., Colombani, N., & Coltorti, M. (2014). Reclamation influence and background geochemistry of neutral saline soils in the Po River Delta Plain (Northern Italy). *Environmental Earth Sciences*, 72(7), 2457–2473. <https://doi.org/10.1007/s12665-014-3154-4>

- Dinelli, E., Tateo, F., & Summa, V. (2007). Geochemical and mineralogical proxies for grain size in mudstones and siltstones from the Pleistocene and Holocene of the Po River alluvial plain, Italy. In J. Arribas, M. J. Johnsson, & S. Critelli (Eds.), *Sedimentary provenance and petrogenesis: Perspectives from petrography and geochemistry*. Geological Society of America. [https://doi.org/10.1130/2007.2420\(03\)](https://doi.org/10.1130/2007.2420(03))
- D.Lgs n. 152/2006. (2006). *Norme in materia ambientale. GU Serie Generale n.88 del 14-04-2006 - Suppl. Ordinario n. 96, Pub. L. No. 152. D. Lgs n. 152/2006*. Retrieved from <https://www.gazzettaufficiale.it/dettaglio/codici/materiaAmbientale>
- Du Laing, G., De Vos, R., Vandecasteele, B., Lesage, E., Tack, F. M. G., & Verloof, M. G. (2008). Effect of salinity on heavy metal mobility and availability in intertidal sediments of the Scheldt estuary. *Estuarine, Coastal and Shelf Science*, 77(4), 589–602. <https://doi.org/10.1016/j.ecss.2007.10.017>
- Falconer, K. E. (1998). Managing diffuse environmental contamination from agricultural pesticides: An economic perspective on issues and policy options, with particular reference to Europe. *Agriculture, Ecosystems & Environment*, 69(1), 37–54. [https://doi.org/10.1016/S0167-8809\(98\)00095-4](https://doi.org/10.1016/S0167-8809(98)00095-4)
- Fernández-Caliani, J. C., Giráldez, M. I., Waken, W. H., Del Río, Z. M., & Córdoba, F. (2021). Soil quality changes in an Iberian pyrite mine site 15 years after land reclamation. *Catena*, 206, 105538. <https://doi.org/10.1016/j.catena.2021.105538>
- Ferraro, A., Parisi, A., Barbone, E., Race, M., Mali, M., Spasiano, D., & Fratino, U. (2022). Characterising contaminants distribution in marine-coastal sediments through multivariate and nonparametric statistical analyses: A complementary strategy supporting environmental monitoring and control. *Environmental Monitoring and Assessment*, 195(1), 59. <https://doi.org/10.1007/s10661-022-10617-4>
- Filippini, M., Zanotti, C., Bonomi, T., Sacchetti, V., Amorosi, A., Dinelli, E., & Rotiroli, M. (2021). Deriving natural background levels of arsenic at the meso-scale using site-specific datasets: An unorthodox method. *Water*, 13(4), 452. <https://doi.org/10.3390/w13040452>
- Franks, M., Duncan, E., King, K., & Vázquez-Ortega, A. (2021). Role of Fe- and Mn-(oxy)hydroxides on carbon and nutrient dynamics in agricultural soils: A chemical sequential extraction approach. *Chemical Geology*, 561, 120035. <https://doi.org/10.1016/j.chemgeo.2020.120035>
- Franzini, M., Leoni, L., & Saitta, M. (1972). A simple method to evaluate the matrix effects in X-Ray fluorescence analysis. *X-Ray Spectrometry*, 1(4), 151–154. <https://doi.org/10.1002/xrs.1300010406>
- Friedland, G., Grüneberg, B., & Hupfer, M. (2021). Geochemical signatures of lignite mining products in sediments downstream a fluvial-lacustrine system. *Science of the Total Environment*, 760, 143942. <https://doi.org/10.1016/j.scitotenv.2020.143942>
- Gadde, R. R., & Laitinen, H. A. (1974). Heavy metal adsorption by hydrous iron and manganese oxides. *Analytical Chemistry*, 46(13), 2022–2026. <https://doi.org/10.1021/ac60349a004>
- Gattaceca, J. C., Vallet-Coulomb, C., Mayer, A., Claude, C., Radakovitch, O., Conchetto, E., & Hamelin, B. (2009). Isotopic and geochemical characterization of salinization in the shallow aquifers of a reclaimed subsiding zone: The southern Venice Lagoon coastland. *Journal of Hydrology*, 378(1–2), 46–61. <https://doi.org/10.1016/j.jhydrol.2009.09.005>
- Gharaibeh, M. A., Marschner, B., Heinze, S., & Moos, N. (2020). Spatial distribution of metals in soils under agriculture in the Jordan Valley. *Geoderma Regional*, 20, e00245. <https://doi.org/10.1016/j.geodrs.2019.e00245>
- Ghezzi, L., Buccianti, A., Giannecchini, R., Guidi, M., & Petrini, R. (2021). Geochemistry of mine stream sediments and the control on potentially toxic element migration: A case study from the Baccatoio Basin (Tuscany, Italy). *Mine Water and the Environment*, 40(3), 722–735. <https://doi.org/10.1007/s10230-021-00789-9>
- Giambastiani, B. M. S., Colombani, N., Mastrociccio, M., & Fidelibus, M. D. (2013). Characterization of the lowland coastal aquifer of Comacchio (Ferrara, Italy): Hydrology, hydrochemistry and evolution of the system. *Journal of Hydrology*, 501, 35–44. <https://doi.org/10.1016/j.jhydrol.2013.07.037>
- Giambastiani, B. M. S., Greggio, N., Carloni, G., Molducci, M., & Antonellini, M. (2023). Geochemical data of bottom sediments from a network of drainage canals located in the low-lying coastal area of Ravenna, Italy [Dataset]. *Zenodo*. <https://doi.org/10.5281/zenodo.8098993>
- Giambastiani, B. M. S., Greggio, N., Nobili, G., Dinelli, E., & Antonellini, M. (2018). Forest fire effects on groundwater in a coastal aquifer (Ravenna, Italy). *Hydrological Processes*, 32(15), 2377–2389. <https://doi.org/10.1002/hyp.13165>
- Giambastiani, B. M. S., Kidanemariam, A., Dagneu, A., & Antonellini, M. (2021). Evolution of salinity and water table level of the phreatic coastal aquifer of the Emilia Romagna Region (Italy). *Water*, 13(3), 372. <https://doi.org/10.3390/w13030372>
- Giambastiani, B. M. S., Macciocca, V. R., Molducci, M., & Antonellini, M. (2020). Factors affecting water drainage long-time series in the salinized low-lying coastal area of Ravenna (Italy). *Water (Switzerland)*, 12(1), 256. <https://doi.org/10.3390/w12010256>
- Giller, K. E., Witter, E., & Mcgrath, S. P. (1998). Toxicity of heavy metals to microorganisms and microbial processes in agricultural soils: A review. *Soil Biology and Biochemistry*, 30(10–11), 1389–1414. [https://doi.org/10.1016/S0038-0717\(97\)00270-8](https://doi.org/10.1016/S0038-0717(97)00270-8)
- Greggio, N., Giambastiani, B. M. S., & Antonellini, M. (2018). Infiltration/irrigation trench for sustainable coastal drainage management: Emilia-Romagna (ITALY). *Environmental Engineering and Management Journal*, 17(10), 2379–2390. <https://doi.org/10.30638/eeemj.2018.236>
- Greggio, N., Giambastiani, B. M. S., Campo, B., Dinelli, E., & Amorosi, A. (2018). Sediment composition, provenance, and Holocene paleo-environmental evolution of the Southern Po River coastal plain (Italy). *Geological Journal*, 53(3), 914–928. <https://doi.org/10.1002/gj.2934>
- Greggio, N., Giambastiani, B. M. S., Mollema, P., Laghi, M., Capo, D., Gabbianelli, G., et al. (2020). Assessment of the main geochemical processes affecting surface water and groundwater in a low-lying coastal area: Implications for water management. *Water*, 12(6), 1720. <https://doi.org/10.3390/w12061720>
- Guo, H., Zhang, B., Li, Y., Berner, Z., Tang, X., Norra, S., & Stüben, D. (2011). Hydrogeological and biogeochemical constraints of arsenic mobilization in shallow aquifers from the Hetao basin, Inner Mongolia. *Environmental Pollution*, 159(4), 876–883. <https://doi.org/10.1016/j.envpol.2010.12.029>
- Hackney, C. T., & Avery, G. B. (2015). Tidal wetland community response to varying levels of flooding by saline water. *Wetlands*, 35(2), 227–236. <https://doi.org/10.1007/s13157-014-0597-z>
- Hammer, Ø., Harper, D. A. T., & Ryan, P. D. (2001). PAST: Paleontological statistics software package for education and data analysis (Vol. 4(1), p. 9).
- Hassaan, M. A., El-Rayis, O., Hemada, E., & El Nemr, A. (2022). Assessment of potentially toxic elements in water and sediments in the drainage network of Lake Mariout, Egypt. *SN Applied Sciences*, 4(8), 239. <https://doi.org/10.1007/s42452-022-05123-8>
- Hua, K., Wang, T., Guo, Z., Zhan, L., He, C., & Wang, D. (2023). Accumulation of potentially toxic elements under long-term application of different organic amendments. *Nutrient Cycling in Agroecosystems*, 126(2–3), 293–309. <https://doi.org/10.1007/s10705-023-10293-x>
- Jia, Y., Guo, H., Xi, B., Jiang, Y., Zhang, Z., Yuan, R., et al. (2017). Sources of groundwater salinity and potential impact on arsenic mobility in the western Hetao Basin, Inner Mongolia. *Science of the Total Environment*, 601–602, 691–702. <https://doi.org/10.1016/j.scitotenv.2017.05.196>
- Kelderman, P., Drossaert, W. M. E., Min, Z., Galione, L. S., Okonkwo, L. C., & Clarisse, I. A. (2000). Pollution assessment of the canal sediments in the city of Delft (The Netherlands). *Water Research*, 34(3), 936–944. [https://doi.org/10.1016/S0043-1354\(99\)00218-3](https://doi.org/10.1016/S0043-1354(99)00218-3)
- Kralj, M. (2012). *Effects of resources exploitation on water quality: Case studies in salt water intrusion and acid mine drainage*. PhD thesis. University of Bologna. Retrieved from <http://amsdottorato.unibo.it/4812/>

- Leoni, L., & Saitta, M. (1976). X-Ray fluorescence analysis of 29 trace elements in rock and mineral standards. *Rendiconti Soc. Italiana Mineralogia e Petrologia*, 32(2), 497–510.
- Manceau, A., Charlet, L., Boisset, M. C., Didier, B., & Spadini, L. (1992). Sorption and speciation of heavy metals on hydrous Fe and Mn oxides. From microscopic to macroscopic. *Applied Clay Science*, 7(1–3), 201–223. [https://doi.org/10.1016/0169-1317\(92\)90040-T](https://doi.org/10.1016/0169-1317(92)90040-T)
- Mao, L., Kong, H., Li, F., Chen, Z., Wang, L., Lin, T., & Lu, Z. (2022). Improved geochemical baseline establishment based on diffuse sources contribution of potential toxic elements in agricultural alluvial soils. *Geoderma*, 410, 115669. <https://doi.org/10.1016/j.geoderma.2021.115669>
- Marconi, V., Antonellini, M., Balugani, E., & Dinelli, E. (2011). Hydrogeochemical characterization of small coastal wetlands and forests in the Southern Po plain (Northern Italy). *Ecohydrology*, 4(4), 597–607. <https://doi.org/10.1002/eco.204>
- Mastrocicco, M., Colombani, N., Di Giuseppe, D., Faccini, B., & Coltorti, M. (2013). Contribution of the subsurface drainage system in changing the nitrogen speciation of an agricultural soil located in a complex marsh environment (Ferrara, Italy). *Agricultural Water Management*, 199, 144–153. <https://doi.org/10.1016/j.agwat.2012.12.018>
- Mastrocicco, M., Colombani, N., Di Giuseppe, D., Faccini, B., Ferretti, G., & Coltorti, M. (2016). Abnormal trace element concentrations in a shallow aquifer belonging to saline reclaimed environments, Codigoro (Italy). *Rendiconti Lincei*, 27(1), 95–104. <https://doi.org/10.1007/s12210-015-0454-x>
- Mastrocicco, M., Giambastiani, B. M. S., & Colombani, N. (2012). Ammonium occurrence in a salinized lowland coastal aquifer (Ferrara, Italy). *Hydrological Processes*, 27(24), 3495–3501. <https://doi.org/10.1002/hyp.9467>
- Migani, F., Borghesi, F., & Dinelli, E. (2015). Geochemical characterization of surface sediments from the northern Adriatic wetlands around the Po river delta. Part I: Bulk composition and relation to local background. *Journal of Geochemical Exploration*, 156, 72–88. <https://doi.org/10.1016/j.gexplo.2015.05.003>
- Mollema, P. N., Antonellini, M., Dinelli, E., Gabbianelli, G., Greggio, N., & Stuyfzand, P. J. (2013). Hydrochemical and physical processes influencing salinization and freshening in Mediterranean low-lying coastal environments. *Applied Geochemistry*, 34, 207–221. <https://doi.org/10.1016/j.apgeochem.2013.03.017>
- Mollema, P. N., Antonellini, M., Dinelli, E., Greggio, N., & Stuyfzand, P. J. (2015). The influence of flow-through saline gravel pit lakes on the hydrologic budget and hydrochemistry of a Mediterranean drainage basin. *Limnology & Oceanography*, 60(6), 2009–2025. <https://doi.org/10.1002/lno.10147>
- Nieder, R., & Benbi, D. K. (2023). Potentially toxic elements in the environment – A review of sources, sinks, pathways and mitigation measures. *Reviews on Environmental Health*, 0(0), 0161. <https://doi.org/10.1515/reveh-2022-0161>
- Orecchia, C., Giambastiani, B. M. S., Greggio, N., Campo, B., & Dinelli, E. (2022). Geochemical characterization of groundwater in the confined and unconfined aquifers of the Northern Italy. *Applied Sciences*, 12(15), 7944. <https://doi.org/10.3390/app12157944>
- Orhue, E. R., & Frank, U. O. (2011). Fate of some heavy metals in soils: A review. *Journal of Applied and Natural Science*, 3(1), 131–138. <https://doi.org/10.31018/jans.v3i1.171>
- Paalman, M. A. A., van der Weijden, C. H., & Loch, J. P. G. (1994). Sorption of cadmium on suspended matter under estuarine conditions: Competition and complexation with major seawater ions. *Water, Air, and Soil Pollution*, 73(1), 49–60. <https://doi.org/10.1007/BF00477975>
- Pavoni, E., Covelli, S., Adami, G., Baracchini, E., Cattelan, R., Crosera, M., et al. (2018). Mobility and fate of Thallium and other potentially harmful elements in drainage waters from a decommissioned Zn-Pb mine (North-Eastern Italian Alps). *Journal of Geochemical Exploration*, 188, 1–10. <https://doi.org/10.1016/j.gexplo.2018.01.005>
- Petrini, R., Pennisi, M., Vittori Antisari, L., Cidu, R., Vianello, G., & Aviani, U. (2014). Geochemistry and stable isotope composition of surface waters from the Ravenna plain (Italy): Implications for the management of water resources in agricultural lands. *Environmental Earth Sciences*, 71(12), 5099–5111. <https://doi.org/10.1007/s12665-013-2913-y>
- Piacentini, T., Galli, A., Marsala, V., & Miccadei, E. (2018). Analysis of soil erosion induced by heavy rainfall: A case study from the NE Abruzzo hills area in Central Italy. *Water*, 10(10), 1314. <https://doi.org/10.3390/w10101314>
- Poto, L., Gabrieli, J., Crowhurst, S., Agostinelli, C., Spolaor, A., Cairns, W. R. L., et al. (2015). Cross calibration between XRF and ICP-MS for high spatial resolution analysis of ombrotrophic peat cores for palaeoclimatic studies. *Analytical and Bioanalytical Chemistry*, 407(2), 379–385. <https://doi.org/10.1007/s00216-014-8289-3>
- Pourret, O., & Hursthouse, A. (2019). It's time to replace the term “heavy metals” with “potentially toxic elements” when reporting environmental research. *International Journal of Environmental Research and Public Health*, 16(22), 4446. <https://doi.org/10.3390/ijerph16224446>
- Protano, G., Di Lella, L. A., & Nannoni, F. (2021). Exploring distribution of potentially toxic elements in soil profiles to assess the geochemical background and contamination extent in soils of a metallurgical and industrial area in Kosovo. *Environmental Earth Sciences*, 80(15), 486. <https://doi.org/10.1007/s12665-021-09771-8>
- Prudêncio, M. I., Valente, T., Marques, R., Sequeira Braga, M. A., & Pamplona, J. (2015). Geochemistry of rare Earth elements in a passive treatment system built for acid mine drainage remediation. *Chemosphere*, 138, 691–700. <https://doi.org/10.1016/j.chemosphere.2015.07.064>
- Ravenscroft, P., Brammer, H., & Richards, K. (2009). *Arsenic pollution - A global synthesis*. Wiley-Blackwell. <https://doi.org/10.1002/9781444308785>
- Reimann, C., & De Caritat, P. (1998). *Chemical elements in the environment*. Springer Berlin Heidelberg. <https://doi.org/10.1007/978-3-642-72016-1>
- RER. (1999). Note illustrative della Carta Geologica D'Italia alla scala 1:50000, foglio 219 Sassuolo (p. 197).
- RER - Emilia-Romagna Region. (1999). *Geological map of the Emilia-Romagna plain*. S.E.I.C.A.
- Richard, F. C., & Bourg, A. C. M. (1991). Aqueous geochemistry of chromium: A review. *Water Research*, 29(7), 807–816. [https://doi.org/10.1016/0043-1354\(91\)90160-r](https://doi.org/10.1016/0043-1354(91)90160-r)
- Rotiroli, M., Jakobsen, R., Fumagalli, L., & Bonomi, T. (2015). Arsenic release and attenuation in a multilayer aquifer in the Po Plain (Northern Italy): Reactive transport modeling. *Applied Geochemistry*, 63, 599–609. <https://doi.org/10.1016/j.apgeochem.2015.07.001>
- Sacchi, E., Brenna, S., Fornelli Genot, S., Leoni, A., Sale, V. M., & Setti, M. (2020). Potentially toxic elements (PTEs) in cultivated soils from Lombardy (Northern Italy): Spatial distribution, origin, and management implications. *Minerals*, 10(4), 298. <https://doi.org/10.3390/min10040298>
- Sall, M. L., Diaw, A. K. D., Gningue-Sall, D., Efremova Aaron, S., & Aaron, J.-J. (2020). Toxic heavy metals: Impact on the environment and human health, and treatment with conducting organic polymers, a review. *Environmental Science and Pollution Research*, 27(24), 29927–29942. <https://doi.org/10.1007/s11356-020-09354-3>
- Salminen, R., Batista, M. J., Bidovec, M., Demetriades, A., De Vivo, B., De Vos, W., et al. (2005). Geochemical atlas of Europe. Part 1 – Background information, methodology and maps. (FOREGS). Retrieved from <http://weppi.gtk.fi/publ/foregsatlas/index.php>
- Sánchez-Donoso, R., García Lorenzo, M. L., Esbrí, J. M., García-Noguero, E. M., Higuera, P., & Crespo, E. (2021). Geochemical characterization and trace-element mobility assessment for metallic mine reclamation in soils affected by mine activities in the Iberian Pyrite Belt. *Geosciences*, 11(6), 233. <https://doi.org/10.3390/geosciences11060233>

- Shi, Z., Blake, W. H., Wen, A., Chen, J., Yan, D., & Long, Y. (2021). Channel erosion dominates sediment sources in an agricultural catchment in the Upper Yangtze basin of China: Evidence from geochemical fingerprints. *Catena*, *199*, 105111. <https://doi.org/10.1016/j.catena.2020.105111>
- Soboyejo, L. A., Giambastiani, B. M. S., Molducci, M., & Antonellini, M. (2021). Different processes affecting long-term Ravenna coastal drainage basins (Italy): Implications for water management. *Environmental Earth Sciences*, *80*(15), 493. <https://doi.org/10.1007/s12665-021-09774-5>
- Soliman, N. F., Younis, A. M., & Elkady, E. M. (2019). An insight into fractionation, toxicity, mobility and source apportionment of metals in sediments from El Tamsah Lake, Suez Canal. *Chemosphere*, *222*, 165–174. <https://doi.org/10.1016/j.chemosphere.2019.01.009>
- Srarfi, F., Rachdi, R., Bol, R., Gocke, M. I., Brahim, N., & SlimShimi, N. (2019). Stream sediments geochemistry and the influence of flood phosphate mud in mining area, Metlaoui, Western south of Tunisia. *Environmental Earth Sciences*, *78*(6), 211. <https://doi.org/10.1007/s12665-019-8215-2>
- Stančić, Z., Fiket, Ž., & Vuger, A. (2022). Tin and antimony as soil pollutants along railway lines—A case study from North-Western Croatia. *Environments*, *9*(1), 10. <https://doi.org/10.3390/environments9010010>
- Stockdale, A., Davison, W., Zhang, H., & Hamilton-Taylor, J. (2010). The association of cobalt with iron and manganese (oxyhydr)oxides in marine sediment. *Aquatic Geochemistry*, *16*(4), 575–585. <https://doi.org/10.1007/s10498-010-9092-1>
- Świetlik, R., Trojanowska, M., Strzelecka, M., & Bocho-Janiszewska, A. (2015). Fractionation and mobility of Cu, Fe, Mn, Pb and Zn in the road dust retained on noise barriers along expressway – A potential tool for determining the effects of driving conditions on speciation of emitted particulate metals. *Environmental Pollution*, *196*, 404–413. <https://doi.org/10.1016/j.envpol.2014.10.018>
- Teatini, P., Ferronato, M., Gambolati, G., Bertoni, W., & Gonella, M. (2005). A century of land subsidence in Ravenna, Italy. *Environmental Geology*, *47*(6), 831–846. <https://doi.org/10.1007/s00254-004-1215-9>
- Toller, S., Funari, V., Zannoni, D., Vasumini, I., & Dinelli, E. (2022). Sediment quality of the Ridracoli fresh water reservoir in Italy: Insights from aqua regia digestion and sequential extractions. *Science of the Total Environment*, *826*, 154167. <https://doi.org/10.1016/j.scitotenv.2022.154167>
- U.S. EPA. (2007a). Method 3051A (SW-846): Microwave assisted acid digestion of sediments, sludges, and oils," revision 1. Washington, DC. Retrieved from <https://www.epa.gov/sites/default/files/2015-12/documents/3051a.pdf>
- U.S. EPA. (2007b). Method 7473 (SW-846): Mercury in solids and solutions by thermal decomposition, amalgamation, and atomic absorption spectrophotometry," revision 0. Washington, DC. Retrieved from <https://www.epa.gov/sites/default/files/2015-07/documents/epa-7473.pdf>
- U.S. EPA. (2018). Method 6010D (SW-846): Inductively coupled plasma-optical emission spectrometry," revision 5. Washington, DC. Retrieved from <https://www.epa.gov/sites/default/files/2015-12/documents/6010d.pdf>
- Vareda, J. P., Valente, A. J. M., & Durães, L. (2019). Assessment of heavy metal pollution from anthropogenic activities and remediation strategies: A review. *Journal of Environmental Management*, *246*, 101–118. <https://doi.org/10.1016/j.jenvman.2019.05.126>
- Viadero, R. (2019). The geochemistry of acid mine drainage. In P. Maurice (Ed.), *Encyclopedia of water* (1st ed., pp. 1–8). Wiley. <https://doi.org/10.1002/9781119300762.wsts0133>
- Weī, L., Liu, Y., Cai, D., Li, F., Luo, D., Li, D., et al. (2022). River morphology redistributes potentially toxic elements in acid mine-drainage-impacted river sediments: Evidence, causes, and implications. *Catena*, *214*, 106183. <https://doi.org/10.1016/j.catena.2022.106183>
- Weiske, A., Schaller, J., Hegewald, T., Kranz, U., Feger, K.-H., Werner, I., & Dudel, E. G. (2013). Changes in catchment conditions lead to enhanced remobilization of arsenic in a water reservoir. *Science of the Total Environment*, *449*, 63–70. <https://doi.org/10.1016/j.scitotenv.2013.01.041>
- Weissengruber, L., Möller, K., Puschenreiter, M., & Friedel, J. K. (2018). Long-term soil accumulation of potentially toxic elements and selected organic pollutants through application of recycled phosphorus fertilizers for organic farming conditions. *Nutrient Cycling in Agroecosystems*, *110*(3), 427–449. <https://doi.org/10.1007/s10705-018-9907-9>
- Wenzel, W. W., Kirchbaumer, N., Prohaska, T., Stingeder, G., Lombi, E., & Adriano, D. C. (2001). Arsenic fractionation in soils using an improved sequential extraction procedure. *Analytica Chimica Acta*, *436*(2), 309–323. [https://doi.org/10.1016/S0003-2670\(01\)00924-2](https://doi.org/10.1016/S0003-2670(01)00924-2)
- WHO. (2017). *Guidelines for drinking-water quality* (4th ed.). World Health Organization.